EXPERIMENTAL EVALUATION OF A PURGED SUBSTRATE MULTILAYER INSULATION SYSTEM FOR LIQUID HYDROGEN TANKAGE

by Richard L. DeWitt and Max B. Mellner

Lewis Research Center
Cleveland, Ohio 44135

NATIONAL AERONAUTICS AND SPACE ADMINISTRATION • WASHINGTON, D. C. • MAY 1971

1. Report No.	2. Government Accession No.	3. Recipient's Catalog No.
NASA TN D-6331		

4. Title and Subtitle: EXPERIMENTAL EVALUATION OF A PURGED SUBSTRATE MULTILAYER INSULATION SYSTEM FOR LIQUID HYDROGEN TANKAGE

5. Report Date: May 1971

6. Performing Organization Code:

7. Author(s): Richard L. DeWitt and Max B. Mellner

8. Performing Organization Report No.: E-6036

9. Performing Organization Name and Address:
Lewis Research Center
National Aeronautics and Space Administration
Cleveland, Ohio 44135

10. Work Unit No.: 180-31

11. Contract or Grant No.:

12. Sponsoring Agency Name and Address:
National Aeronautics and Space Administration
Washington, D.C. 20546

13. Type of Report and Period Covered: Technical Note

14. Sponsoring Agency Code:

15. Supplementary Notes:

16. Abstract

Seven space-hold and six ground-hold tests were conducted to determine the thermal performance of a GHe purged substrate multilayer blanket insulation system on a 7-ft- (2.134-m-) diam. spherical LH_2 tank. Space-hold tests were made using 30, 40, 50, and 60 insulation shields. No serious degradation of the space-hold thermal performance of the 30 layer system was observed over consecutive cyclic tests. The space-hold performance was found to be a strong function of the technique of application. The main source of unexpected heat leak during ground hold was believed due to condensing and freezing of nitrogen in the insulation blankets.

17. Key Words (Suggested by Author(s))	18. Distribution Statement
Thermal insulation; Liquid hydrogen; Thermal conductivity; Conductive heat transfer; Thermal degradation; Temperature effects; Heat shielding; Temperature control; Thermocouples; Pressure chambers; Pressure gages; Control equipment; Vacuum chambers	Unclassified - unlimited

19. Security Classif. (of this report)	20. Security Classif. (of this page)	21. No. of Pages	22. Price*
Unclassified	Unclassified	65	$3.00

*For sale by the National Technical Information Service, Springfield, Virginia 22151

CONTENTS

EXPERIMENTAL EVALUATION OF A PURGED SUBSTRATE MULTILAYER INSULATION SYSTEM FOR LIQUID HYDROGEN TANKAGE

by Richard L. DeWitt and Max B. Mellner
Lewis Research Center

SUMMARY

In the field of insulation study insufficient attention has been paid to determination of the thermal performance of large scale liquid hydrogen (LH_2) tank mounted systems. The work reported herein is an experimental determination of both the space-hold and the ground-hold performance of a gaseous helium (GHe) purged substrate multilayer blanket insulation system for a 7-foot- (2.134-m-) diameter spherical LH_2 tank. The work was conducted in a 25-foot- (7.620-m-) diameter spherical side loading vacuum chamber. No isothermal shroud was employed around the test configuration. The heat source was the ambient temperature chamber wall.

The objectives of the seven space-hold tests were to determine (1) if repeated thermal cycling of the system would cause degradation of the performance, (2) the reproducibility of the thermal performance after removal, inspection, and reinstallation of the insulation blankets, and (3) determination of the performance of the insulation system for three, four, five, and six blanket thicknesses (i.e., 30, 40, 50, and 60 radiation shields). Five additional tests were made to determine the ground-hold performance.

No serious degradation of the space-hold thermal performance of the three-blanket system was observed over three consecutive cyclic tests. The space-hold performance of the three-blanket system was found, however, to be a strong function of the technique of application. Heat flux values of 0.373 and 0.579 Btu per hour per square foot (4.233×10^3 and 6.571×10^3 J/(hr)(m^2)) for the originally installed and reinstalled systems, respectively. For the four-, five-, and six-blanket tests the total heat flux through the undisturbed insulation system decreased approximately proportional to the thickness of the insulation.

All the boiloff rates measured during the ground-hold tests were considered in excess of what they should have been had this subsystem performed as originally designed. The main source of unexpected heat addition to the test tank was believed due to condensing and freezing of nitrogen in the insulation blankets.

INTRODUCTION

The use of liquid hydrogen (LH_2) as a propellant for near earth and lunar spacecraft requires well designed thermal protection systems to minimize bulk heating and/or phase change of the fuel. These systems must be capable of thermally isolating the fuel tank from its surroundings during ground hold, boost, and finally, some given space-hold period such as interplanetary transfer and/or planetary orbit.

The insulation system configurations which are presently being used and those planned for the future can be divided arbitrarily into those sufficient for short term missions (say $\leq$8 days) and systems for interplanetary travel (>8 days). Numerous analytical and experimental investigations have been conducted for both tank mounted and shadow shield insulation systems for each of the two categories of missions. The bulk of the work reported in the literature deals with the "first step" (i. e., tank mounted insulation systems for short term missions). The majority of the experimental work which is reported has been accomplished using calorimeter-type test equipment. The general objective has been to obtain total heat flux data through insulation samples as a function of the following parameters: shield coating, spacer material, packing density, and boundary temperature. These experiments have generally been closely controlled and have been directed at determining the lowest possible heat flux values obtainable. Much screening of insulation system configurations, as well as specific engineering design information has resulted from this work. A comprehensive summary of insulation technology advances is available as reference 1.

One objective that has not received much attention is the thermal performance of large scale tank mounted insulation systems which (1) have been exposed to several thermal cycles prior to launch or (2) have had to be partially removed at the launch pad to effect some tank or fluid component repair before start of the mission. Further, since predictability of large scale tank mounted insulation system performance is still somewhat of an art, the technology could be improved by deterining the thermal performance of the given system as a function of the number of shields.

The work described in this report deals with additional space-hold and ground-hold thermal performance of a purged substrate multilayer blanket insulation system which was originally designed for an 82. 6-inch- (2. 098-m-) diameter spherical LH_2 tank undergoing an 8-day lunar mission. This system was originally tested under simulated ground-hold and space-hold environmental thermal conditions (NASA contract NAS 3-4199). The original investigators obtained heat flux rates of 18 000 and 165. 6 Btu per hour (18.98×10^6 and 0.174×10^6 J/hr) for a single ground-hold and space-hold test, respectively. Temperature measurements obtained during the test work indicated that the ground-hold protection portion of the system was inadequate. Further, the temperature measurements indicated that a significant improvement in the space-hold performance could probably be obtained by removing the fiberglass girth strip at the support cone-

to-tank junction and replacing the strip with multilayer blankets. Complete test results are presented in reference 2. No comparison of the data from reference 2 with the data of this report will be made because of the difference in test conditions employed.

The multilayer insulation system, as originally conceived, consisted of a 0.5-inch- (0.0127-m-) thick fiberglass mat sublayer covered by 30 layers of multilayer insulation (0.25-mil or 6.35×10^{-6}-m Mylar coated both sides with vapor deposited aluminum) fabricated in gore-shaped blankets. The multilayer insulation was separated from the fiberglass mat sublayer by a plastic vapor barrier.

During the ground-hold period, the fiberglass mat sublayer was purged with gaseous helium (GHe) and the blankets were exposed to gaseous nitrogen (GN_2). The purpose of the GHe was to purge all condensibles from the sublayer and also to keep the surface of the plastic vapor barrier above the condensation temperature of the GN_2 in the blankets.

The purpose of the multilayer insulation blankets was to serve as the primary protection against the radiation heat transfer encountered during space hold. Each blanket of insulation consisted of ten double-aluminized Mylar radiation shields, each separated by a glass fiber paper spacer. Nylon monofilament threads and Teflon buttons were utilized to assemble the ten radiation shields and nine paper spacers in each of the three modular blankets.

The objectives of this present work were fourfold: (1) to determine if repeated thermal cycling of the insulation system would cause degradation of the space-hold performance of the tank mounted insulation system, (2) determine the reproducibility of the thermal performance after removal, inspection, and reinstallation of the insulation blankets, (3) determine the space-hold performance of the insulation system for three, four, five, and six blankets, and (4) determine the performance of the ground-hold subsystem.

All tests were conducted in a 25-foot- (7.620-m-) diameter spherical, side loading, vacuum chamber. No isothermal shroud was employed around the test configuration. The heat source was the ambient temperature chamber wall. The view factor of the test configuration to the vacuum chamber wall was essentially 1.0. Liquid hydrogen was the propellant used in all test runs.

For the space-hold portion of the program, seven tests were conducted. The first three tests were simple thermal cyclic tests on the three-blanket configuration (i.e., the insulation was cooled from room temperature to its operating temperature and then allowed to return to room temperature). The three insulation blankets on the tank hemispheres and support cone were then carefully removed, inspected, and reinstalled before the fourth test (objective 2) was conducted. The last three tests were made with four, five, and six insulation blankets (nominally 40, 50, and 60 shields), respectively.

Six ground-hold tests also were conducted. Five of the tests were made with GHe in the substrate and GN_2 in the insulation blankets. The final test was made with GHe in both the substrate and the insulation blankets.

The propellant ullage level in all tests was kept between 4 and 16 percent. Total heat flux into the propellant was obtained by measuring the boiloff gas flow rate. Temperature profiles, thermophysical property data, and transport property data were then used to calculate the various components of the total heat flux.

SYMBOLS

A	area, ft^2; m^2
B	heat lost to ullage gas by one liquid-level sensor, Btu/sec; J/sec
C	heat lost to liquid propellant by one liquid-level sensor, Btu/sec; J/sec
CF	coefficient of discharge
c_p	specific heat at constant pressure, Btu/(lb)(^oR); J/(kg)(K)
D	diameter, in.; m
DINSUL	internal energy change of insulation system, Btu/sec; J/sec
DTANK	internal energy change of tank wall, Btu/sec; J/sec
DULL	internal energy change of tank ullage gas, Btu/sec; J/sec
F	conversion factor in eq. (13)
h	specific enthalpy, Btu/lb; J/kg
i	number of liquid-level sensors in ullage
j	index number
K	specific heat ratio
k	thermal conductivity, Btu/(hr)(ft)(^oR); J/(hr)(m)(K)
k_{eff}	effective thermal conductivity, Btu/(hr)(ft)(^oR); J/(hr)(m)(K)
L	length or thickness, ft; m
l	index number
M	mass, lb; kg
$\dot{M}$	mass flow rate, lb/sec; kg/sec
m	index number
n	number of effective radiation shields
P	pressure, psia; N/m^2 abs
PTANK	tank pressure, psia; N/m^2 abs

Q	heat flow, Btu/hr; J/hr
Q_b	heat transferred across insulation boundary, Btu/sec; J/sec
QCONE	heat conducted into propellant through support cone, Btu/sec; J/sec
QINSUL	heat flux through insulation system on both hemispheres and both hats, Btu/sec; J/sec
QLLS	heat lost to propellant by liquid-level sensors, i(B) + (13 - i)C, Btu/sec; J/sec
QOUT	latent and sensible heat contained in boiloff gas, Btu/sec; J/sec
QPIPES	heat conducted into tank through service lines, Btu/sec; J/sec
QPSMI	QINSUL ± DINSUL, Btu/sec; J/sec
QPURGE	heat lost to propellant by ground-hold helium purge gas, Btu/sec; J/sec
QUNINT	heat flow through insulation system covering tank hemispheres only, Btu/sec; J/sec
QWIRES	heat conducted into insulation through instrumentation wires, Btu/sec; J/sec
q	heat flux, Q/A, Btu/(hr)(ft^2); J/(hr)(m^2)
R	universal gas constant, ft-lbf/(lbm)(^oR); J/K
T	temperature, ^oR; K
TEW	environmental chamber wall temperature, ^oR; K
ΔT	temperature differential, ^oR; K
t	time, sec
Δu	internal energy change, Btu/sec; J/sec
V	volume, ft^3; m^3
$\dot{V}$	volumetric flow, ft^3/sec; m^3/sec
Δ	indicates differential
ϵ	emissivity
λ	latent heat of evaporation, Btu/lb; J/kg
ρ	density, lb/ft^3; kg/m^3
σ	Stephan-Boltzmann constant, 1.713×10^{-9} Btu/(hr)(ft^2)($^oR^4$); J/(hr)(m^2)(K^4)
$\dot{\omega}$	flow rate, lb/sec; kg/sec

Subscripts:

B	blanket

BO	boiloff
C	complete thickness of blankets and substrate
COMP	component
GHe	gaseous helium
H	free hemispherical area of tank
IDEAL	theoretical radiation heat flux through insulation blankets
IN	in
LIQ	saturated liquid
m	index
OSM	outside surface of insulation, measured
OUT	out
PM	propellant, measured
s	shield
VAP	saturated vapor
VL	position on vent line where insulation intersects
W	wall

INSULATION SYSTEM

A detailed description of the design, fabrication, and installation of the three-blanket insulation system is given in reference 2. Therefore, the description of the system will only be summarized in this report.

The basic test configuration consisted of (1) an 82.6-inch- (2.098-m-) diameter spherically shaped test tank, (2) a continuous support cone, and (3) an Aclar purge bag enclosed fiberglass mat sublayer covered by 30 layers of multilayer insulation.

Figure 1 is a veiw of the test tank and support cone. The tank hemispheres, Y-ring, and access port cover were constructed of 2219-T87 aluminum. Nominal tank wall thickness was 0.125 inch (0.0032 m). The continuous support cone was constructed of 0.016-inch- (0.0004-m-) thick 6Al-2.5Sn titanium. Molded fiberglass covers were used to contain both the personnel access hatch and the sump at the base of the tank. Portions of these covers were removable to allow access to seals and instrumentation lines with only a minimum of interruption of the insulation. Figure 1 also shows the first step of the installation which was the cementing of Velcro fasteners to the outside

surface of the tank and cone. This set of fasteners was used to both attach and support the fiberglass sublayer.

The second step was the addition of the 0.5-inch- (0.0127-m-) thick fiberglass mat sublayer (fig. 2) to both tank hemispheres as well as the outside of the support cone. This mat was then covered by an Aclar bag. The substrate and Aclar bag on the top hemisphere were not interconnected with any of the software on the bottom hemisphere because of the support cone. A view of the installation of the sublayer and the Aclar bag arrangement, at least on the bottom hemisphere, can be seen in figure 2. The complete installation of the sublayer and the Aclar bag constituted the helium purged ground-hold system. The objectives of using the helium purge gas were to remove condensibles in the sublayer and to maintain the Aclar bag (on the outside of the fiberglass sublayer) at a temperature $\geq 140^{\circ}$ R (77.8 K), the condensation temperature of GN_2. Gaseous nitrogen was used as the multilayer insulation blanket purge since it has a lower thermal conductivity than GHe and hence is desirable to reduce the gaseous hydrogen (GH_2) boil-off during the ground-hold condition. Four helium purge gas paths were used. They are shown schematically in figure 3.

Three insulation blankets were applied over the Aclar purge bags (fig. 4). Each blanket of insulation consisted of ten double-aluminized Mylar radiation shields (0.25-mil (6.35×10^{-6}-m) Mylar coated both sides with vapor deposited aluminum), each separated by a 2.8-mil- (71.12×10^{-6}-m-) thick glass fiber paper spacer (Dexiglas). Monofilament threads and Teflon buttons were utilized to assemble the ten radiation shields and nine Dexiglas spacers of each blanket into the gore-shaped modules (see fig. 5(a)). Velcro fasteners were used to attach the gore segments of the inner blanket to the Aclar purge bag. The second blanket was supported by nylon threads which were first tied behind the buttons on the inside surface of the second blanket. The threads were then tied beneath selected buttons on the first blanket (see fig. 5(b)). The third blanket was tied to the second blanket in the same manner. A nylon net was used as the outermost covering of the test configuration.

The fourth, fifth, and sixth blankets were individually installed on the top hemisphere in the same manner as the second and third. The extra blankets on the bottom hemisphere were individually supported by means of integral nylon straps attached to the top of the cone support and the sump cover-to-tank intersection (fig. 6). Actual weights of the substrate and all insulation blankets are listed in table I.

The only major change between this system and the original installation (i.e., NASA contract NAS 3-4199) was in the support cone-to-tank junction area. The original fiberglass girth strip was deleted and three blankets of multilayer insulation were used instead as per the recommendation made in reference 2.

TEST FACILITY

Figure 7 shows the test tank suspended inside the 25-foot- (7.62-m-) diameter environmental test chamber. A 6-inch- (0.125-m-) high aluminum facility channel ring was attached to the top of the test tank titanium support cone to assure uniform load distribution. Three 3/8-inch- (0.0095-m-) diameter stainless steel rods were used to hang the test configuration from the overhead rails inside the chamber. The facility chamber was capable of maintaining a vacuum of $\approx 1\times10^{-5}$ mm Hg during space-hold operation.

Figure 8 is a general schematic of the facility plumbing. The four major subsystems are (1) the fill line cold guard, (2) the vent line backpressure control system, (3) the helium substrate purges, and (4) the nitrogen atmosphere control required for ground hold.

During all test periods, a manually adjusted active flow of LH_2 was kept up in the fill line downstream of the tank shutoff valve. This flow served to minimize any heat leak up the fill line to the tanked propellant.

Two parallel flow paths in the vent line outside the environmental chamber (1) allowed filling of the test tank without over-ranging the volumetric boiloff meters and (2) allowed the boiloff gas to warm to ambient temperature before passing through the boiloff meters.

A major piece of equipment in the vent line was the tank backpressure valve and its associated control equipment. This unit controlled tank pressure to approximately 16.5 psi (113.76×10^3 N/m^2) within ±0.0036 psi (±24.82 N/m^2) during space-hold tests and ±0.0014 psi (±9.65 N/m^2) during ground-hold tests. This bandwidth was calculated using the data obtained by monitoring the output signal of the high resolution tank pressure sensor in the backpressure control circuit. Inasmuch as any loss of tank pressure increases the vent line flow rate and, conversely, any increase in tank pressure results in a decreased boiloff flow, the extreme importance of a fine resolution backpressure circuit cannot be overemphasized by the authors. The resolution necessary can be calculated once the approximate boiloff rate and the allowable error in that rate have been specified.

Figure 9 is a block diagram of the tank backpressure control circuit used during this test program. The critical component of the circuit was the high resolution differential pressure transducer. The particular transducer employed had an advertised resolution of $\pm1\times10^{-5}$ mm Hg. This unit sensed any differential pressure between the test tank and some constant pressure held in a reference bottle located in a temperature conditioned bath outside the environmental chamber. (An ice water bath was selected to house the reference volume bottle because this type of bath had the least temperature change for the range of barometric pressure values expected during testing.) The output of the differential pressure transducer was electrically conditioned and used as an

input signal to the controller of a valve in the tank vent line. Since a large difference existed between the ground-hold and space-hold boiloff rates, two separate controllers and valves were used.

The four separate helium gas substrate purges were individually controllable. A choked flow orifice in each line enabled measurement of the flow rate. Also, during ground-hold testing, the environmental chamber was filled in a controlled manner with either GN_2 or GHe. A relief valve in the chamber vent line prevented chamber pressure from rising more than 0.180 psi (1.241×10^3 N/m^2) above atmospheric pressure.

INSTRUMENTATION

The basic objective of the instrumentation was to provide enough temperature data so all solid conduction heat fluxes, as well as internal energy changes of the insulation, tank, ullage, and liquid propellant could be determined. A second objective was to determine the mass rate of flow and energy level of the vent gases.

Both simple and differential thermocouples as well as platinum resistance temperature sensors comprised the temperature transducers on the test configuration. The platinum sensors were generally used where good accuracy at low absolute values was required (e.g., the tank wall, the tank vent line, the liquid fill line, etc.). Thermocouples were employed where temperatures $\geq 100^{\circ}$ R (55.56 K) were expected. The differential thermocouples were used in several instances to help reduce the number of instrumentation lead wires, and their associated heat flows, to the test configuration.

Figure 10 is a schematic of the instrumentation on the test package. A typical cross section of an installation on the top hemisphere consisted of (1) two platinum resistance temperature sensors on the tank wall, (2) three copper-constantan (Cu-Cn) differential measurements from the outside surface of the third blanket to (a) the Aclar bag, (b) the outside surface of the first blanket, and (c) the outside surface of the second blanket, (3) an absolute temperature measurement of the outer surface of the third blanket (Cu-Cn thermocouple), and (4) absolute surface temperature measurements for the outer surfaces of blankets 4, 5, and 6 (Chromel-constantan (Cr-Cn) thermocouples).

The only difference in the temperature instrumentation on the bottom hemisphere was that thermocouples were employed instead of platinum resistance sensors on the tank wall. These thermocouples were used for general monitoring, not as a source of prime data.

Two groups of radial temperature measurements were also installed at the girth of the test tank. The titanium support cone and the Y-ring were instrumented with both platinum resistance sensors and thermocouples. The tank lid, as well as both the vent and fill lines, were instrumented with platinum resistance temperature sensors. The tank vent line also contained one platinum resistance sensor and a thermocouple for

measurement of boiloff gas temperature. The heat flux through the helium gas substrate purge lines and the instrumentation lines coming in the top hat and sump cover were determined using Cr-Cn thermocouples. Platinum resistance sensors were used on the ends of the helium purge lines inside the fiberglass covers in order to obtain an exact temperature of the gas during ground-hold tests. Bonded strain-gage transducers were used to measure the tank pressure, the pressure in the LH_2 fill line, and the inlet pressure of the ground-hold GHe substrate purge. A rotating vane flowmeter was used to monitor filling of the test tank and also the LH_2 flow when the fill line cold guard system was operational.

An effort was made in both the top hat and the sump cover areas to obtain a measure of any interaction between the insulation blankets and the main tank service lines (i. e., vent and fill lines). Differential Cu-Cn thermocouple junctions were installed within the first three blankets; Cr-Cn couples were mounted on the fourth, fifth, and sixth blankets. Intermittent difficulty (mainly open differential measurements) was encountered with the signals obtained from both sets of the differential measurements during all space-hold tests. The data from these junctions served only to evaluate changes in the internal energy of the insulation. These particular measurements were not completely usable for their primary objective.

Internal tank instrumentation consisted of six platinum temperature sensors and thirteen hot wire liquid-level probes. The temperature sensors were used to obtain propellant and ullage gas temperatures; the liquid-level sensors were used to obtain discrete liquid-level positions during the tank load and the test period.

Two differential volumetric gas flowmeters were used to measure the boiloff gas flow rate. The range of the low flow unit was 0 to 75 SCFH (0 to 2. 12 m^3/hr); the range for the meter used during ground-hold testing was 0 to 23 000 SCFH (0 to 651. 3 m^3/hr). Standard Cu-Cn thermocouples and bonded strain-gage pressure sensors were used directly upstream of each meter.

The GHe substrate purge flow rates were monitored by using four separate 0. 0135-inch- (0.343×10^{-3}-m-) diameter jeweled orifices. Flow through the orifices was always choked; four separate strain-gage pressure transducers were located directly upstream of the orifices.

Figure 11(a) shows an electrolytic copper distribution plate and associated lead wires used for the differential thermocouple measurements. The illustration is labeled in order that use of the disk in obtaining the measurements may be understood. Figure 11(b) is a schematic of how the sensing junction of each thermocouple was attached to either the Alcar bag or the double-aluminized Mylar. In all cases, the leads from any sensing element installation were taped along a shield for a distance not less than 12 inches (0. 305 m). All insulated leads from the thermocouples were a maximum of 10 mils (0.254×10^{-3} m) in diameter; platinum resistor leads were 20 mils (0.508×10^{-3} m) in diameter.

PROCEDURE

Space-Hold Testing

The first step of the procedure for space-hold testing was to evacuate the 25-foot-(7.62-m-) diameter environmental chamber to a vacuum of approximately 1×10^{-5} mm Hg. The warm test tank and insulation system were cooled as the tank was filled with LH_2 against a controlled backpressure of at least 19 psia (131×10^3 N/m^2 abs). The decreasing boiloff flow rate was only roughly monitored by splitting the flow between the space-hold meter and the main tank vent line. Intermittent topping of the tank was continued during an additional insulation cooling period after the fill. Once the boiloff was within the range of the space-hold meter, the topping process was discontinued and the tank shutoff valve was closed. The fill line cold guard subsystem was put into operation by opening the cold guard vent valve. The tank was then slowly vented (using the main tank vent line) to the desired run pressure. This operation served to release the excess sensible heat in the tanked liquid and also served to preclude any stratification by mixing the propellant. The tank backpressure control was then put into operation.

Two deviations in this procedure were experienced in space-hold tests 3-1 and 3-3. In test 3-1, a controlled backpressure was not kept on the tank during the initial fill. As a result, the liquid was not saturated at the start of the data recording period. The outcome of this deviation will be elaborated on in the RESULTS AND DISCUSSION section. In test 3-3, the procedure started with a filled tank in a 1-atmosphere GHe environment. This step had to be taken because in previous 1-atmosphere-level tests, GN_2 had condensed and frozen on the partially insulated propellant tank fill lines inside the vacuum chamber. Subsequent chamber pumpdown was slowed considerably since all the frozen nitrogen had to sublime in the process. This sublimation resulted in a high throughput of gas in the facility diffusion pumps which, in turn, tended to overheat and cause a run shutdown. Because of the higher thermal conductivity of GHe, considerably more topping of the tank was required while the environmental chamber was being pumped down. When the chamber reached $\approx1\times10^{-5}$ mm Hg, the test setup procedure continued normally.

Ground-Hold Testing

Two test techniques were employed. The first started with a warm test tank and insulation system in a 1-atmosphere air environment. The chamber was then purged with GN_2 or GHe to remove air and the GHe substrate purges were initiated. The test tank was filled using the throttling valve on the tank main vent line to maintain a controlled backpressure. The tank was topped as required during the insulation system

cooling process. Once the boiloff was within range of the boiloff meter, the topping process was stopped, the cold guard subsystem activated, and the tank was slowly vented until the run backpressure control system could be put into operation.

The second procedure started with the tank filled with LH_2 and a vacuum in the environmental chamber. The GHe substrate purges were used to initially break the vacuum; GN_2 was used to complete the process. The entire process was done over a 2-hour time period. The insulation system temperatures were allowed to stabilize while the tank was being topped off against a 19-psia (131×10^3-N/m^2 abs) backpressure. Once system temperatures had become fairly stable, the cold guard subsystem was initiated, the tank was vented, and the backpressure control system was put into operation.

The first procedure was used when the ground-hold test period was the only test to be conducted. The second procedure was employed when a space-hold test immediately preceded a ground-hold period.

DATA REDUCTION

Basic Equations

The basic procedure used was to subtract all solid conduction heat flows, as well as internal energy changes of the insulation, tank, ullage, and liquid propellant from the heat equivalent of the gross boiloff value of the insulated tank. The net boiloff value obtained gave the heat flow through the insulation system on both hemispheres and both hats.

Figure 12 is a schematic representation of the heat vectors which were evaluated. The approximate location of where each vector was evaluated as well as a cutaway view of the insulation system tank wall combination are also shown on the figure.

To simplify the data reduction, an insulation boundary was drawn between the insulation system and the test tank wall. Considering the volume inside the boundary (i. e., tank wall and contents), the following energy summation may be written:

$$Q_b = QOUT + DULL \bullet |DTANK| - QLLS \qquad (1)$$

Q_b	QOUT	DULL	$\bullet \lvert DTANK \rvert$	QLLS
heat transferred across insulation boundary	latent and sensible heat conduction in boiloff gas	internal energy change of ullage gas	internal energy change of tank wall	heat lost to propellant by liquid-level sensors

Heat vectors considered in the volume outside the boundary may, by conservation of energy, be grouped as follows:

Q_b	=	QPURGE	+	QCONE	+	QPIPES	+	QWIRES	+	QPSMI
heat transferred across insulation boundary		heat added by ground-hold helium purge in substrate		heat added by conduction through cone support		heat added by conduction through service lines		heat added by conduction through instrument wires		heat transferred through insulation plus internal energy change of insulation

(2)

A third identity used is

$$\underset{\substack{\text{heat flow through insulation system}}}{\text{QPSMI}} = \underset{\substack{\text{heat flow through insulation system}}}{\text{QINSUL}} \pm \underset{\substack{\text{internal energy change of insulation system}}}{|\text{DINSUL}|} \qquad (3)$$

Equating relations (1) and (2) and substituting equation (3) into the result yield

$$\text{QINSUL} \pm |\text{DINSUL}| = \text{QOUT} + \text{DULL} \pm |\text{DTANK}| - \text{QLLS} - \text{QCONE} - \text{QPIPES} - \text{QWIRES} - \text{QPURGE} \qquad (4)$$

Every term on the right side of the equation, as well as DINSUL, could be experimentally evaluated. The term QINSUL was then obtained directly by subtraction.

It should be noted here that the terms DULL, DINSUL, and DTANK, even though small, will never be zero. Even when steady state exists, there is still some mass leaving the test tank. This loss of mass results in a decreasing liquid level and also causes some small temperature changes in the insulation, the tank ullage, and the tank wall.

Any internal energy change of the liquid propellant is implicit in the DULL and QOUT terms.

Mathematical Representation of Terms in Equation (4)

QOUT. - QOUT is defined as the total latent and sensible heat gained by the liquid propellant boiled off during the boiloff process.

After leaving the test tank and being warmed in the heat exchanger, the vent gas passed through a volumetric flowmeter. Temperature and static pressure transducers were located immediately upstream of the meter. The mass flow rate of gas was determined using the equation

$$\dot{M}_{BO} = \dot{V}_{BO}\rho_{BO} \qquad \text{where } \rho = \rho(P, T) \tag{5}$$

The mass flow rate was determined once every 10 minutes during the entire test period. Values of flow rate between these discrete points were obtained by linear interpolation. The value of QOUT was then calculated by the equation

$$Q_{OUT} = \underbrace{\dot{M}_{BO}\lambda\left(\frac{\rho_{LIQ}}{\rho_{LIQ} - \rho_{VAP}}\right)}_{\text{Latent heat}} + \underbrace{\dot{M}_{BO}(h_{VL} - h_{VAP})}_{\text{Sensible heat}} \tag{6}$$

The factor $\rho_{LIQ}/(\rho_{LIQ} - \rho_{VAP})$ corrects for the vapor that was formed but did not leave the test tank; it merely occupied the space vacated by the evaporated liquid.

DULL. - The term DULL is defined as the internal energy change of the tank ullage gas. The continuous process of boiloff causes some small temperature changes in the ullage which, in turn, cause some change in the internal energy level of the ullage gas.

To determine DULL, the change in liquid level must be determined for each time increment between discrete data points. The liquid level was determined at the start of each test and redetermined at the time the level dropped uncovering a level sensor. The tank volume had previously been calibrated against liquid level and a curve fitted to this calibration. The enthalpy change of the ullage over a time interval t_1 to t_2 may be written

$$\text{DULL} = \frac{\left[\sum_{j=1}^{m+\Delta m} \rho(T)h(T)V_j\right]_{t_2} - \left[\sum_{j=1}^{m} \rho(T)h(T)V_j\right]_{t_1}}{t_2 - t_1} \tag{7}$$

This integral was evaluated at constant pressure using the temperature profile fitted from ullage gas temperature measurements.

DTANK. - The change in energy of the tank wall was determined by applying the first law of thermodynamics to an element of the wall $(M_W)_j$ for a given time interval t_1 to t_2; that is,

$$\text{DTANK} = \left| \frac{\sum_{j=1}^{l} (M_W)_j (c_{p,W})_j (T_2 - T_1)_j}{t_2 - t_1} \right| \tag{8}$$

This numerical integration was performed using the temperature profile fitted to the few temperature sensors on the tank wall, lid, and Y-ring. The index j varied from 5 to 18 depending on the liquid level in the tank.

QLLS. - The energy added to the system by internal instrumentation was solely that of the 13 liquid-level sensors. The rate of heat added when i sensors were in the ullage was

$$\text{QLLS} = (i)B + (13 - i)C \tag{9}$$

where $B = 8.77 \times 10^{-5}$ Btu per second (92.47×10^{-3} J/sec) and $C = 24.6 \times 10^{-5}$ Btu per second (259.37×10^{-3} J/sec). A paragraph on calibration of these sensors appears in the RESULTS AND DISCUSSION section of this report.

QCONE. - The instantaneous heat transfer rate by solid conduction was calculated from the Fourier equation

$$\frac{Q}{A} = -\frac{1}{L} \int_{T_1}^{T_2} k \, dT \tag{10}$$

In numerical integration form, the equation may be written

$$\text{QCONE} = \frac{A}{L} \sum_{j=1}^{m} k_j (T_2 - T_1)_j \qquad \text{where } k = k(T) \tag{11}$$

The integration was performed for two diametrically opposed 4.75-inch- (0.1207-m-) long sections beginning 4.0 inches (0.1016 m) up from the Y-ring-to-cone attachment.

QPIPES. - The piping consisted of the fill line, the vent line, and the helium gas substrate purge lines. The heat flow rate for each of these was computed using a form of equation (11). The integral was taken for a section of line immediately outside the outer surface of the insulation blankets.

QWIRES. - The instrument wiring consisted of leads from thermocouples, platinum resistance temperature sensors, liquid-level sensors, and valve controls. All wiring was attached to associated piping so that the temperature of the pipe and leads could be considered the same. The heat flow rate for each of the bundles of wires was computed using a form of equation (11). Again, the integral was taken for a section of line immediately outside the outer surface of the insulation blankets.

QPURGE. - The energy added by the four helium purges during ground-hold testing was calculated by

$$\text{QPURGE} = \sum_{j=1}^{4} (\dot{M}_{GHe})_j (c_p)_j (T_{IN} - T_{OUT})_j \tag{12}$$

Each helium mass flow rate was determined from a critical flow orifice where

$$\dot{M}_{GHe} = (D^2)(F)(\rho)(CF)\left[RTK\left(\frac{2}{K+1}\right)^{(K+1)/(K-1)}\right]^{1/2} \tag{13}$$

Temperatures and pressure data, for use in the equation, were measured directly upstream of each orifice.

DINSUL. - The change in insulation internal energy was determined by applying the first law of thermodynamics to each component of the system. The system was divided into four components: (1) the top hat consisting of the reinforced fiberglass frame and three insulation blankets, (2) the top hemisphere consisting of the substrate, the Aclar bag, the three insulation blankets on both the hemisphere and the inside surface of the support cone, and any nitrogen gas contained in the blankets during ground-hold testing, (3) the bottom hemisphere consisting of essentially the mirror image of the top hemisphere and, (4) the sump cover consisting of the reinforced fiberglass frame and the three insulation blankets. The numerical integration was done on each component for a given time interval t_1 to t_2 using an equation of the form

$$\text{DINSUL} = \left| \frac{\sum_{j=1}^{l} (M_{COMP})_j (c_{p,\,COMP})_j (T_2 - T_1)_j}{t_2 - t_1} \right| \tag{14}$$

Specific heat values for the double-aluminized Mylar, the Dexiglas, the Aclar purge bag, and the fiberglass substrate were obtained from reference 3.

In equation (3), the term QPSMI represents the heat transferred through the insulation plus the internal energy change of the insulation.

If the insulation was warming (i. e., absorbing heat which would otherwise be flowing to the propellant), the term DINSUL was considered additive to QINSUL in equation (3). Hence, from equation (3)

$$QINSUL = QPSMI - |DINSUL| \tag{15}$$

If the insulation was cooling, this represents a heat addition to the propellant which would not have been present if the insulation temperatures could have been forced to remain constant. Hence, the term DINSUL was defined as detracting from QINSUL in equation (3) and hence

$$QINSUL = QPSMI + |DINSUL| \tag{16}$$

Permutations of Equation (4)

The following equations, (17) to (20), are considered to be the prime data reduction equations. The only reason for having four equations is for convenience in grouping the heat input terms to the LH_2 propellant. The entire group of terms on the left side of each equation is defined to be the prime heat input terms to the propellant for each case considered.

For the case when both the insulation and the tank wall were warming, equation (4) can be written as

$$\underbrace{QINSUL + |DINSUL| + QCONE + QWIRES + QPIPES + QPURGE + QLLS}_{\text{Prime heat input terms}} = QOUT + DULL + |DTANK| \tag{17}$$

For the second case, when the insulation was warming and the tank wall was cooling, the term DTANK was negative and equation (4) was written as

$$\underbrace{QINSUL + |DINSUL| + QCONE + QWIRES + QPIPES + QPURGE + QLLS + |DTANK|}_{\text{Prime heat input terms}} = QOUT + DULL \tag{18}$$

For the third case when the insulation was cooling and the tank wall was warming, the following form of equation (4) is correct:

$$\underbrace{\text{QINSUL} + \text{QCONE} + \text{QWIRES} + \text{QPIPES} + \text{QPURGE} + \text{QLLS}}_{\text{Prime heat input terms}} = \text{QOUT} + \text{DULL} + |\text{DTANK}| - |\text{DINSUL}| \quad (19)$$

Finally, for the case where both the insulation and the tank wall were cooling (i. e., DTANK was negative, equation (4) can be written as

$$\underbrace{\text{QINSUL} + \text{QCONE} + \text{QWIRES} + \text{QPIPES} + \text{QPURGE} + \text{QLLS} + |\text{DTANK}|}_{\text{Prime heat input terms}} = \text{QOUT} + \text{DULL} - |\text{DINSUL}| \quad (20)$$

Heat Leak Through the Uninterrupted Insulation QUNINT

An effort was made to determine the space-hold heat flow through the uninterrupted portion of the insulation (i. e., the heat flow rate through the free hemispherical area of the tank) and to scale up these data to a surrounding temperature of 528° R (293. 3 K). The steps employed are as follows:

(1) The heat flow through the insulation QINSUL was divided evenly into a heat flow through the top and bottom hemispheres. This division was justified since outside average surface temperatures for both hemispheres were with 4° R (2. 2 K) for any given run.

(2) The effects of the radiation and conduction loading, as well as the internal energy changes of the top hat and the sump cover, were removed from the top and bottom hemisphere heat flow values, respectively.

(3) The resulting heat flow values were then divided into an ideal radiation heat transfer component and a solid conduction heat transfer component. The equation used for calculating the ideal radiation component is as follows:

$$q_{IDEAL} = \frac{\sigma\left(T_{OSM}^4 - T_{PM}^4\right)}{n\left(\frac{2}{\epsilon_s} - 1\right)} \quad (21)$$

(4) The radiation components for each hemisphere were scaled up to a boundary temperature of 528° R (293. 3 K) by the ratio

$$\frac{T_{528^{\circ}\,R(293.3\,K)}^4 - T_{PM}^4}{T_{OSM}^4 - T_{PM}^4} \quad (22)$$

This scaling factor assumes that all the radiant energy which reaches the Aclar bag ultimately reaches the liquid propellant.

(5) The solid conduction heat transfer components for each hemisphere were scaled up to a boundary temperature of 528° R (293.3 K) by the ratio

$$\frac{T_{528^{\circ}\ R\ (293.3\ K)} - T_{PM}}{T_{OSM} - T_{PM}} \tag{23}$$

(6) The scaled up values of the heat flows were then normalized for the area of the respective hemispheres to which they pertained.

(7) For each run, the average of the two values of the scaled up heat fluxes (step 6) for each tank hemisphere was then computed.

RESULTS AND DISCUSSION

Space-Hold Testing

General. - In total, seven space-hold tests were conducted. The first three tests were simple cyclic tests to determine if repeated thermal cycling of the insulation system would cause degradation of the space-hold performance. The insulation blankets on the tank hemispheres and support cone were then carefully removed, inspected, and reinstalled before the fourth test was conducted. The last three tests were made with four, five, and six insulation blankets, respectively. For discussion purposes, the data will generally be divided into two groups: the tests on the three-blanket system and the last four "increasing insulation thickness" tests. The rebuilt three-blanket test (R3) is common to both of these groups of data.

Actual boiloff curves obtained. - The original measured boiloff curves obtained are plotted in figures 13 and 14 as a function of test time. Figure 13 displays data for all the three-blanket tests; figure 14 displays data for the increasing insulation thickness tests. The periods of time which are considered to be steady state for each run are tabulated as part of the legend on each plot. It should be pointed out that conclusions should not be drawn at this time using the absolute levels of tank boiloff data shown in figures 13 and 14. The chamber boundary temperatures are different for all tests - these temperatures will be adjusted and the boiloff data will be compared later in the report.

In figure 13, a major difference existed in the transient profile of the boiloff history (preceding steady-state) between test 3-1 and the remaining three tests. This difference was the result of starting test 3-1 with the LH_2 propellant subcooled. As a result,

a good percentage of the heat flux getting into the tank was going into sensible heating of the propellant and not into latent heat of evaporation. Analysis of the data showed that the liquid finally reached a saturated state point after 37 hours of test time. Hence, only the last 2.7 hours of the test were considered to be valid steady-state data. The authors want to emphasize the point that, in any boiloff test, the liquid propellant must be saturated and maintained at a constant pressure before the boiloff rate reflects the true heat flux into the test tank.

A second singularity in figure 13 appears as a peak in the boiloff history of test 3-2. The explanation for this was simply a short term loss of LH_2 in the fill line cold guard subsystem. The fast rise rate in boiloff for the short term loss of LH_2 flow in the fill line cold guard subsystem can be construed as a verification of saturated liquid propellant in the test tank.

Also, it should be noted that the cooldown characteristics of the insulation system can and do change as a function of variables such as tank fill rate, initial environmental chamber pressure level, and initial start temperature of the insulation. These parameters were not the same for each test and hence different boiloff rates were observed for the different tests prior to the steady-state periods. These different transient time histories do not in any way affect the steady-state test results and hence were not of prime concern to the authors. Also in figure 13, a large difference existed between the boiloff of test R3 and the results obtained from the first three tests. This difference, which will be discussed in detail later in the report, was due basically to the stripping and reinstallation of the multilayer blankets.

In figure 14, a singularity occurred during the test on the five-blanket system. Analysis of the data revealed that no mechanical malfunction had occurred. It is the opinion of the authors that the slight dropoff, rise, and return to steady state of the boiloff history was due to a very localized and transient superheating condition which occurred in the test tank. The total energy involved in the small dip preceding the sharp rise in boiloff was very small (1 Btu or 1.05×10^3 J maximum). This energy is matched by the area under the very short, very sharp, rise of the boiloff history curve. After the stored energy was released, the boiloff rate returned to 1.6 percent of its steady-state value.

The actual GH_2 boiloff data for the end of test 4 are shown below that of the end of test 5. This apparent anomaly can be accounted for by the inability to control the variations in environmental chamber wall temperature from test to test. The environmental chamber was approximately 20° F (11.1 K) higher in test 5 than in test 4. Later discussion will show that this fact more than accounts for the apparent reversed positions of these two tests.

The remaining singularity in figure 14 was the period of time during the six-blanket tests when the internal tank liquid-level sensors were intentionally turned off to cali-

brate the quantity of heat they were releasing to the liquid propellant. This singularity will be discussed in the following section.

Calibration of internal tank liquid-level sensors. - As mentioned in the INSTRUMENTATION section, there were 13 hot wire liquid-level sensors located inside the test tank. Inasmuch as these units were adding heat to the ullage gas and the LH_2 propellant during all tests, a calibration of the heat addition was necessary. The exact calibration to use was determined during testing of the six-blanket configuration. After 13 hours of steady-state boiloff had been obtained, the power to all sensors was shut off for a period of 3 hours (note the step change in the curve in fig. 14). The change in boiloff was 310×10^{-5} Btu per second (3.268 J/sec). The sensors were then turned back on and voltage and current data were recorded for one sensor in the ullage and two submerged in the liquid. The power being dissipated by the sensor in the ullage was 8.77×10^{-5} Btu per second (92.47×10^{-3} J/sec); the average power being dissipated by the sensors in the liquid was 24.6×10^{-5} Btu per second (259.37×10^{-3} J/sec). Applying these results to all the sensors in both the ullage and the liquid propellant yielded a value of 288×10^{-5} Btu per second (3.037 J/sec) being added by the instrumentation for the six-blanket system test. The difference between the actual change in boiloff measured and the computed heat input by the instrumentation was

$$\frac{310\times10^{-5}\ \text{Btu/sec} - 288\times10^{-5}\ \text{Btu/sec}}{310\times10^{-5}\ \text{Btu/sec}} \times 100 = \frac{3.268\ \text{J/sec} - 3.037\ \text{J/sec}}{3.268\ \text{J/sec}} \times 100 = 7.1\ \text{percent}$$

Since the agreement obtained between the predicted and experimental values was so close, the term QLLS was determined for each test using calculated values of energy.

Division of the prime heat input into the insulated tank. - A tabulation of the absolute values of all the heat flows into the LH_2 propellant as well as all the hardware internal energy changes is presented in table II.

Percentages of the prime heat input for each test have been calculated and are plotted in figure 15. For all tests the following generalities are noted:

(1) Less than 3 percent of the heat was coming in through the plumbing connections.

(2) Between 20 and 27 percent was coming in through the cone support.

(3) Between 9 and 14 percent was coming in through the thermocouple and platinum resistance temperature probe lead wires.

(4) Between 7 and 10 percent was being added by the internal tank hot wire sensors.

In summary, if exact values from table II are used, between 37 and 52 percent of the total heat input to the propellant was due to the presence of the instrumentation or hardware connections to the test tank. Hence, between 48 and 62 percent of the heat input to the propellant was transmitted by the insulation blankets, coming through them by

radiation and solid conduction. It should also be noted that the percentage of heat transmitted through the blankets was not a strong function of the number of layers of insulation.

Overall insulation system efficiency. - A comparison was made between the empirically obtained heat flow through the insulation system QINSUL and the ideal value obtained from theory. The ideal radiation heat transfer through the effective number of radiation shields n was calculated for each run by the following equation:

$$Q_{IDEAL} = \frac{A\sigma\left(T_{OSM}^4 - T_{PM}^4\right)}{n\left(\frac{2}{\epsilon_s} - 1\right)} \qquad \text{where } \epsilon = 0.026$$

The ideal radiation percentage of the heat coming through the insulation system was then computed and is plotted in figure 16. These results show that all the configurations tested were only between 10 and 15 percent efficient as radiation insulation systems (i. e., if all solid conduction through the insulation system could be eliminated, the performance of the configuration could be improved by a factor between 6. 7 to 10. 0). It should also be noted in the figure that the ideal radiation percentage is almost constant over the "increasing insulation thickness" tests. Disregarding the slightly different test boundary temperatures, this fact implies that the total heat flow through the insulation system decreased approximately proportional to the thickness of the insulation (i. e., as "n" was increased, Q_{IDEAL} decreased. The fact that the ratio Q_{IDEAL}/QINSUL remained constant implies that QINSUL decreased approximately proportional to "n.").

In summary then, figure 17, which is a complete apportionment of the absolute values of the heat flows into the LH_2 propellant, was obtained by superimposing the result of figure 16 on figure 15.

Heat flux through the uninterrupted insulation. - The technique of calculation of the heat flux through the uninterrupted portion of the insulation for both actual test temperatures and 528° R (293. 3 K) boundary temperatures was detailed in the DATA REDUCTION section. All values used and resulting from these calculations are shown in table III.

Figure 18 is a plot of both the original and the scaled values of heat flux through the uninterrupted portion of the insulation for each run.

The arithmetic average of the scaled heat fluxes for the first three tests was 0. 373 Btu per hour per square foot (4.233×10^3 J/(hr)(m^2)). The value obtained for the first test was only 0. 5 percent below this average. Test 3-2, the second of the series, showed a decrease of 7. 77 percent. The result of the third test was a value 8. 2 percent

above the average. The engineering conclusion drawn is that no serious degradation of the space-hold thermal performance of this insulation system was observed for the three tests conducted.

The result of the reinsulated tank test (R3) was that the heat flux increased by 55.4 percent relative to the average of the first three cyclic tests. This fact leads to the conclusion that the space-hold performance, or efficiency, of this insulation system was definitely a strong function of details of the technique of application. The two qualitative reasons offered as explanation for this increased boiloff rate are (1) a net compression of the insulation blankets resulting from the second installation, and (2) an increase visually observed in the number of gaps at seams between abutting insulation blankets after reinstallation.

The scaled test data for the "increasing insulation thickness" tests are also plotted in figure 18. The trend displayed is that the boiloff rate tends to decrease approximately linearly with increasing insulation thickness. It should be noted here that the results for the four- and five-blanket configurations (0.381 Btu/(hr)(ft^2) or 4.324×10^3 J/(hr)(m^2) and 0.360 Btu/(hr)(ft^2) or 4.086×10^3 J/(hr)(m^2), respectively) are almost identical with the resulting average of the first three cyclic tests (0.373 Btu/(hr)(ft^2) or 4.233×10^3 J/(hr)(m^2)). In order that no false conclusions are drawn because of this anomaly, it must be stated that the only test results which may be directly compared are as follows: (1) any comparison of tests within the first three cyclic tests, (2) comparison of any or all of the three cyclic tests with the reinstalled insulation system test, and (3) any comparison of tests within the "increasing insulation thickness" series.

If the fourth, fifth, and sixth blankets had been added to the original three-blanket systems, the authors fully expect the resultant heat leak through the uninterrupted portion of the insulation would have decreased from the 0.373 Btu per hour per square foot (4.233×10^3 J/(hr)(m^2)) average of the first three cyclic tests just as it did from the 0.579 Btu per hour per square foot (6.571×10^3 J/(hr)(m^2)) value of the reinsulated tank test.

The insulation system was X-rayed after the first group of cyclic tests as well as after each of the tests in the "increasing insulation thickness" series. Three photographs were taken near each of the two radial temperature profile instrumentation positions on both the top and bottom hemispheres. Small diameter lead (i.e., Pb) wires had been laid on the surface of each blanket in an effort to determine individual blanket thicknesses. The overall thickness values of the entire set of radiation blankets were easily measured. Determination of individual blanket thicknesses, however, was difficult because the indicator wires were not lined up exactly on a tank hemisphere radius vector. The data obtained from these measurements on the top and bottom hemispheres are plotted in figures 19 and 20, respectively. Prior to reinstallation of the multilayer blankets, the sublayer was fluffed on both hemispheres. On the top hemisphere, the insulation blanket thickness was compressed by 13.2 percent as a result of the reinstallation.

On the bottom hemisphere, the overall multilayer blanket thickness was reduced by 53.1 percent. Since the space-hold performance of this type of insulation system has been shown by previous investigators to be very load sensitive (ref. 4), the increase in boiloff observed for the rebuilt system is understandable.

Quantitative evaluation of the increased number of gaps at seams between abutting insulation blankets for the two different three-blanket systems was difficult. For this reason, the increase in observed gaps (approximately $\leq 1/16$ in. or 0.0016 m) is offered only as a qualitative fact to help explain the increased boiloff rate of the reinstalled insulation system. The major cause of the increased boiloff is still considered to be the excessive compression observed after the insulation blankets had been reinstalled.

Insulation system temperature profiles. - It is concluded that the seven insulation configurations under test performed poorly when viewed only from a radiation heat transfer standpoint. One of the major indications of the predominant type of heat transfer through the insulation systems is the type of radial temperature profile observed. Figures 21 and 22 are plots of measured steady-state temperatures in the top hat, top and bottom hemispheres, and the sump cover. In figure 21 are displayed data for all the three-blanket tests; figure 22 displays data for the "increasing insulation thickness" tests.

For all tests conducted, the temperature profiles in both the top hat and sump cover are fairly linear indicating predominantly solid conduction-type heat transfer through the insulation blankets. To obtain a qualitative appreciation of this fact, an analytically predicted temperature profile for radiation heat transfer was calculated for both the top hat and hemisphere areas. These curves were added to figure 21 only for reference. For all three-blanket tests, the temperature profiles in the top hemisphere indicate a slight digression from pure solid conduction. This trend, however, disappeared as the fourth, fifth, and sixth blankets were added and the gradients were close to linear.

In the bottom hemisphere insulation, the temperature profiles tended more toward a radiation profile for the three-blanket system than in the top hemisphere. Figure 22, however, displays almost a complete return to the solid conduction-type profile after reinstallation of the system and during the entire "increasing insulation thickness" tests. In figure 21, the bottom hemisphere temperature profile for the reinstalled three-blanket configuration shows the result of the 53.1 percent reduction in insulation thickness. The profile is almost linear. Also, a sharp discontinuity is evident in the slope of the temperature profiles for the bottom hemisphere at the Aclar purge bag. This discontinuity was present for the reinstalled three-blanket configuration as well as for the four-, five-, and six-blanket tests. It is believed by the authors that this sharp discontinuity was caused because the resistance to heat flow was primarily in the insulation itself and not in the fiberglass substrate. Hence the discontinuity is a function of the spacing of

the Aclar bag from the surface of the tank. If the sagging had not occurred, this discontinuity would not have been as pronounced.

The point alluded to by these data is that packing density changes of the magnitude produced by manual installation definitely influenced the temperature profiles through the insulation and thereby increased the conduction component of heat transfer through the insulation. (Packing densities of the insulation for all tests are shown in table IV for quantitative reference.) As previously mentioned, this relation between packing density and insulation heat flux has been brought out by other investigators. It is discussed here only to display the general agreement between the results of these tests and some of the previous test work on insulation systems.

Effective conductivity. - A term found in the literature to describe the usefulness of an insulation system is "effective conductivity." This value is computed as follows:

$$k_{eff} = \frac{(QUNINT)L_B}{A_H \Delta T}$$

Using the temperature values plotted in figures 21 and 22 and the individual heat fluxes through the insulation computed in step 6 of the section Heat Leak Through the Uninterrupted Insulation QUNINT, the effective conductivities of the blankets for each of the seven space-hold tests were calculated. The results for both the top and bottom hemispheres are shown in figures 23 and 24. These results will not be discussed in detail; however, two observations can be drawn from these figures. The first is that, at any given temperature, the spread in effective conductivity is as much as a factor of four. The second observation is that the effective thermal conductivity increases with increasing blanket temperature. This fact implies that even if one could be sure of the absolute magnitude of the effective conductivity for one given temperature, a pronounced error in any tank boiloff prediction could be expected due to the temperature dependency of this parameter.

Further, it should be appreciated that there are at least four major variables which contributed directly to the heat flux through the insulation blankets of this system. These factors are (1) insulation packing density, (2) residual noncondensible gases trapped between the radiation shields, (3) any condensed gases between the shields, and (4) nonreproducibility of insulation installation. To evaluate the exact effect of these parameters is, at best, exceedingly difficult.

In addition, the heat transfer process through multilayer insulation system is not that of solid conduction - a fact which presupposes nonlinear temperature profiles in the insulating shields.

In conclusion, then, the authors wish to point out that the aforementioned reasons are inadequacies which must be considered when trying to use the term "effective con-

ductivity" to predict space-hold propellant boiloff values for an insulation system. It is obvious that the definition of effective conductivity does not take them into account.

Comparison of full-scale insulation performance data with calorimeter data. - Further experimental tests to gain additional information on the performance of an insulation system which duplicated the three-blanket system of this report have recently been completed at Lewis Research Center (ref. 5). One of the basic objectives of this work was to obtain a steady-state heat flux value through the insulation system at a simulated space-hold condition.

The test tank employed in this work was a 65-inch- (1.65-m-) diameter by 89.5-inch- (2.28-m-) long double guarded cylindrical calorimeter. The space-hold performance value obtained was 0.301 Btu per hour per square foot (3.416×10^{3} J/(hr)(m^2)). This value is plotted in figure 25 along with the results of all seven tests of this report. The agreement of data from the two programs is considered good.

Plumbing penetrations. - As listed in table II and portrayed in figure 17, the heat flow down all the plumbing penetrations amounted to less than 3 percent of the total heat flow into the insulated tank. An attempt was made during the four-blanket test to determine how much interaction was occurring between the insulation blankets and the penetrating pipe for the fill line through the bottom sump, and the vent line through the top hat. The heat flow down each pipe was computed for a length of the pipe immediately outside and inside both the sump cover and the top hat.

For the vent line, 0.31×10^{-4} Btu per second (0.0327 J/sec) was flowing toward the vent line top hat intersection in the section of pipe immediately outside the top hat. A flow of 0.29×10^{-4} Btu per second (0.0306 J/sec) was leaving the intersection and flowing towards the manhole cover. The heat lost to the insulation and top hat was 0.02×10^{-4} Btu per second (0.0021 J/sec) or 6.5 percent of the heat coming in through the vent line.

The heat flow values for the fill line were slightly different. In both calculations, heat was flowing down the fill line from the fill line-sump cover intersection. A value of 0.11×10^{-5} Btu per second (0.0012 J/sec) was flowing away from the insulated tank in the section of pipe immediately outside the sump cover; 0.87×10^{-5} Btu per second (0.00917 J/sec) was flowing toward the test tank in the section of pipe immediately inside the sump cover. This peculiar pattern resulted because of the LH_2 cold guard subsystem employed in the fill line.

In both of the previous cases the computed numbers could easily be within the error band of the temperature sensors used in these particular areas. Hence, the engineering conclusion which was drawn is that negligible interaction occurred between the insulation system and the main fill and vent service lines.

Ground-Hold Testing

History. - Performance of the ground-hold subsystem (GHe purged substrate) published in reference 2 showed that the subsystem was not performing as originally designed. The basic trouble was that the fiberglass substrate was not sufficiently thick to maintain a temperature of $\geq 140^{\circ}$ R (77.8 K) on the surface of the Aclar purge bag. As a result, GN_2 was most likely condensing on the purge bag. This point notwithstanding, six ground-hold tests were conducted on the insulated tank to define inadequacies of the subsystem and thereby obtain a better understanding of the difficulties mentioned in reference 2.

Inasmuch as the substrate was thermally inadequate, the analysis and the resulting conclusions reached in this section of the report will be mainly qualitative as opposed to quantitative. For convenience, the history as well as the run setup techniques employed for the ground-hold tests are listed in table V.

Post-test inspection and analysis of ground-hold subsystems. - After all six tests were conducted, the multilayer insulation blankets on the hemispheres were removed. The fiberglass substrate was found to be compressed from an original thickness of 0.5 inch (0.0127 m) to an average thickness of 0.15 inch (0.0038 m) on the top hemisphere and about 0.325 inch (0.0083 m) on the cone and bottom hemisphere (see figs. 19 and 20 in the section Space-Hold Testing). Also, there were tears found in the lower hemisphere purge bag. These tears were such that, during ground-hold testing, they would have allowed some of the helium purge gas to enter the aluminized Mylar blankets. An in-house test (unpublished NASA data from M. P. Hanson) revealed that the Aclar material would contract approximately 1 percent as it was cooled from room temperature to 140° R (77.8 K). This contraction, when applied to the 83.60-inch (2.123-m) outer diameter of the Aclar bag, means that the actual outer diameter would have been 82.76 inches (2.102 m) when the tank was cold. When the contraction of the tank is taken into account, this value of 82.76 inches (2.102 m) represents a compression of 0.257 inch (0.0065 m) on a radius. This fact tends to explain the reduced substrate thickness. It is hypothesized that the thermal contraction of the Aclar also caused the tears in the purge bag.

General remarks. - The total boiloff rates measured for all ground-hold tests are plotted in figure 26. A tabulation of all heat flux components for each of the tests is given in table VI. The data in table VI represent values averaged over the time period between approximately 4 and 16 percent ullage conditions for all runs except run 4. Data for run 4 were taken over the 8 to 12 percent ullage range.

All of the tabulated boiloff rates for the first three tests (GHe in the substrate, GN_2 in the blankets) are suspected of being in excess of what they should have been if the system performed as originally designed. The two reasons for this statement are

(1) that nitrogen was condensing, and in some cases freezing, on the surface of the Aclar bag and inside the blankets and (2) that some GHe was present in the multilayer blankets because of the ruptured Aclar purge bag and because of test setup techniques employed (e.g., breaking the vacuum in the environmental chamber with GHe). The result of the nitrogen condensation and freezing was the addition of both sensible and latent heat to the test tank; the result of GHe in the blankets was an increase in the overall thermal conductivity of the blanket-substrate combination.

Tests conducted in a GN_2 environment. - The first five tests (1, 2, 3a, 3b, and 3c) were conducted in a GN_2 environment. As can be seen in figure 26, two distinct groups of data resulted. The first test (lowest group of data) is considered to be the closest to the true boiloff value; however, the boiloff measured during this test is still high because of the latent and sensible heat added by the condensing and freezing nitrogen. Because of the large difference in boiloff experienced between test 1 and succeeding tests, it was suspected that the purge bag ruptured sometime during test 1. Figure 27 is a plot of the radial temperature gradients measured during test 1 in the insulation system on both the top and bottom hemispheres. One radial gradient in the top hemisphere insulation shows the surface of the Aclar bag at that location to be below the liquifaction point of nitrogen. The two radial profiles in the bottom hemisphere insulation show the Aclar bag temperature to be below the freezing temperature of nitrogen (113° R or 62.78 K). Also, on one side of the bottom hemisphere, the outer surface temperature of the first blanket implies that the entire first blanket was below the liquifaction temperature of nitrogen.

Because of (1) these low temperatures in the insulation blankets and (2) the inexhaustible supply of GN_2 in the environmental chamber, it was concluded that nitrogen condensation was occurring continuously during the testing periods. Most likely more nitrogen would have condensed and frozen on the Aclar bag if the bag had not torn. The torn bag probably allowed some GHe to escape locally into the insulation blankets and displace some of the condensible GN_2. Further evidence of this continuous condensation problem can be obtained by studying figure 28. This figure is a plot of the position averaged radial temperature profiles in the top and bottom hemispheres of the tank for the three ground-hold tests 3a, 3b, and 3c. The bottom hemisphere insulation profiles show a continual cooling through the three tests. The profiles in the top hemisphere also show this trend but not quite as strongly. For test 3a, about 41 percent of the inner blanket on the bottom hemisphere was below the freezing temperature of nitrogen and 79 percent was below the liquifaction temperature. The profiles for the tests 3b and 3c show that 73 percent of the inner blanket on the bottom hemisphere was below the freezing temperature and that the entire inner blanket as well as 14 percent of the middle blanket were below the liquifaction temperature.

To gain a feeling for how much heat could be put into the test tank by the cooling and condensing nitrogen, an arbitrary thickness of 0.1 inch (0.00254 m) of condensed nitrogen was assumed. Over the total hemispherical area of 154.1 square feet (14.32 m^2), a 0.1-inch- (0.00254-m-) thick layer of condensed nitrogen would amount to 1.28 cubic feet (0.0362 m^3). Sensible heat lost by this quantity of nitrogen cooling from 528° to 140° R (293.3 to 77.78 K) would be approximately 617 Btu (0.65×10^6 J); latent heat liberated to the test tank during condensation would be about 5555 Btu (5.86×10^6 J). Total heat addition to the test tank for this example is 6172 Btu (6.51×10^6 J) or, over a 1-hour time period, 1.71 Btu per second (1.803×10^3 J/sec). Relative to tests 3a, 3b, and 3c, this heat leak of 1.71 Btu per second (1.803×10^3 J/sec) which is equivalent to 32.26 pounds per hour (14.633 kg/hr) of boiloff gas would amount to 27, 28, and 28 percent of the QINSUL value shown in table VI. These values are considered to be low since no attempt was made to consider (1) sensible heat lost by the nitrogen between the liquifaction and freezing temperatures, (2) latent heat liberated during freezing, (3) sensible heat lost below the freezing temperature, and (4) the increased thermal conductivity of the frozen layer of nitrogen compared to the thermal conductivity of GN_2.

The conclusion drawn from the foregoing discussion is that the main source of unexpected heat addition to the test tank was due to condensing and freezing of nitrogen in the insulation blankets.

A secondary source of unexpected heat addition to the test tank was probably due to the presence of GHe in the insulation blankets. Ground-hold test 1 was the first thermal cycle imposed on the insulation system. As stated earlier, because of the large difference in boiloff experienced between test 1 and the other four GN_2 tests, it was suspected that the purge bag ruptured sometime during test 1. For tests 2, 3a, 3b, and 3c, the arithmetic temperature average across the blankets (considering both top and bottom insulation profiles) was between 244° and 267° R (135.6 and 148.3 K). Between these temperature limits, the thermal conductivity of GHe is a factor of 5.7 times greater than the thermal conductivity of nitrogen. Since the authors believe that only partial filling of the insulation blankets with helium occurred (also note in table V that the vacuum containing the insulation system was initially broken with GHe), this presence of helium is advanced as the qualitative explanation of why tests 2 to 3c have a higher boiloff rate than test 1.

Test conducted in a GHe environment. - In order to further substantiate the fact the heat flux values obtained in tests 1 to 3c were excessively high, a ground-hold test was conducted with GHe in both the substrate and the insulation blankets. Since both of these volumes were filled with GHe, the purge bag did not have to function as a divider between the substrate and the blankets. Investigation has shown (ref. 3) that during ground hold, the heat transfer through the substrate and the insulation blankets is con-

trolled almost entirely by the gas present in the substrate and blankets. This conclusion was applied against the results of test 4. Since ground-hold heat transfer is essentially by conduction, the total heat flow through only the insulation QINSUL was divided between the hemispheres in a manner inversely proportional to the complete insulation thickness measurements. This division yielded 17 966 Btu per hour (18.94×10^6 J/hr) through the top hemisphere and 9335 Btu per hour (9.84×10^6 J/hr) through the bottom hemisphere. Using the equation

$$k_{GHe} = \frac{(QINSUL)L_C}{A_H \Delta T}$$

and considering the ΔT to exist from the outer surface of the insulation to the tank wall, the conductivities were calculated to be

$$k_{TOP\ HEMISPHERE} = \frac{(17\ 966\ Btu/hr)(0.0692\ ft)}{(75.4\ ft^2)(376^o\ to\ 37^o\ R)} = 0.0487\ Btu/(hr)(ft)(^oR)$$

$$= \frac{(18.94 \times 10^6\ J/hr)(0.0211\ m)}{(7.005\ m^2)(208.9\ to\ 20.56\ K)} = 302.91\ J/(hr)(m)(K)$$

for the upper hemisphere and

$$k_{BOTTOM\ HEMISPHERE} = \frac{(9335\ Btu/hr)(0.1333\ ft)}{(78.7\ ft^2)(398^o\ to\ 37^o\ R)} = 0.0438\ Btu/(hr)(ft)(^oR)$$

$$= \frac{(9.84 \times 10^6\ J/hr)(0.0406\ m)}{(7.311\ m^2)(221.1\ to\ 20.56\ K)} = 272.49\ J/(hr)(m)(K)$$

for the bottom hemisphere. These values are plotted at the arithmetic average of the respective differential temperatures in figure 29. The results of these calculations agree well with the conductivity of pure helium gas. Finally, this agreement tends to support the previous contention that the results of all the GN_2 ground-hold test runs were in excess of what they should have been if the insulation system had performed as originally designed.

SUMMARY OF RESULTS

A total of seven space-hold tests and six ground-hold tests were conducted on a purged substrate multilayer insulation system mounted on a 82.6-inch- (2.098-m-) diameter spherical liquid hydrogen (LH_2) tank. The work was conducted in a 25-foot- (7.62-m-) diameter spherical, side loading, vacuum chamber. No isothermal shroud was employed around the test configuration. The heat source was the ambient temperature chamber wall.

The objectives of this work were fourfold:

(1) To determine if repeated thermal cycling of the insulation system would cause degradation of the space hold performance of the tank-mounted insulation system,

(2) To determine the reproducibility of the thermal performance after removal, inspection, and reinstallation of the insulation blankets,

(3) To determine the space-hold performance of the insulation system for four, five, and six blankets, and

(4) To determine the performance of the ground-hold subsystem.

The results obtained are stated in the following sections.

Space-Hold Tests

1. No serious degradation of the space-hold thermal performance of the three-blanket system was observed over the three cyclic tests performed.

2. The space-hold performance, or efficiency, of the three-blanket system was definitely a strong function of the technique of application. Heat flux values of 0.373 and 0.5797 Btu per hour per square foot (4.233×10^3 and 6.571×10^3 J/(hr)(m^2)) were obtained for the originally installed and the reinstalled systems, respectively.

3. The total heat flux through the undisturbed insulation system decreased approximately proportional to the thickness of the insulation.

4. Between 37 and 52 percent of all the heat input to the propellant was transmitted by the insulation blankets or was coming through them by radiation and solid conduction. The remainder was due to the continuous cone tank support, instrumentation lead-in wires, internal tank instrumentation, and plumbing connections.

5. All the configurations tested were between 10 and 13.3 percent efficient as radiation insulation systems. If all solid conduction through the insulation system could be eliminated, the performance of the configuration can be improved by a factor between 6.7 and 10.0.

6. Insulation packing density definitely influences the temperature profiles through the insulation and thereby increases the conduction component of heat transfer through the insulation.

7. The term "effective conductivity" is not a truly independent and meaningful parameter to use when predicting space-hold propellant boiloff values for this multilayer insulation system.

8. The agreement of insulation heat flux data between this program and a concurrent in-house investigation by Sumner and Maloy of a configuration duplicating the three-blanket system was found to be good.

9. Negligible interaction occurred between the insulation system and the test tank fill and vent service lines.

Ground-Hold Tests

1. All of the measured boiloff rates (for the conditions of gaseous helium (GHe) in the substrate and gaseous nitrogen (GN_2) in the blankets) are considered in excess of what they should have been had the system performed as originally designed.

2. The main source of unexpected heat addition to the test tank was believed due to condensing and freezing of nitrogen in the insulation blankets.

3. Unpurged GHe in the insulation blankets was a secondary source of the unexpectedly high ground-hold heat flow obtained for four of the six test cycles. Some of the GHe entered the insulation blankets as a result of tears in the Aclar purge bag.

4. Successful use of GN_2 open purges around a LH_2 tank is very difficult.

Lewis Research Center,
National Aeronautics and Space Administration,
Cleveland, Ohio, January 14, 1971,
180-31.

REFERENCES

1. Glaser, Peter E.; Black, Igor A.; Lindstrom, Richard S.; Ruccia, Frank E.; and Wechsler, Alfred E.: Thermal Insulation Systems, A Survey. NASA SP-5027, 1967.

2. Sterbentz, W. H.; and Baxter, J. W.: Thermal Protection System for a Cryogenic Spacecraft Propulsion Module. Vol. II. Rep. LMSC-A794993, Lockheed Missiles and Space Co. (NASA CR-54879, vol. 2), Nov. 15, 1966.

3. Coston, R. M.: Handbook of Thermal Design Data for Multilayer Insulation Systems. Vol. II. Rep. LMSC-A847882. Lockheed Missiles and Space Co. (NASA CR-87485), June 25, 1967.

4. Anon.: Advanced Studies on Multi-Layer Insulation Systems. Rep. ADL-67180-00-04, Arthur D. Little, Inc. (NASA CR-54929), June 1, 1966.

5. Sumner, Irving E.; and Maloy, Joseph E.: Transient Thermal Performance of Multilayer Insulation Systems During Simulated Ascent Pressure Decay. NASA TN D-6335, 1971.

6. Johnson, Victor J.: A Compendium of the Properties of Materials at Low Temperature (Phase I). Part I. Properties of Fluids. Cryogenic Eng. Lab., National Bureau of Standards (WADD TR 60-56, pt. 1), July 1960.

TABLE I. - WEIGHT AND AREA SUMMARY

Position of insulation	Fiberglass substrate	Aclar bag	Inner blanket	Second blanket	Third blanket	Fourth blanket	Fifth blanket	Sixth blanket	Surface area, ft^2 (m^2)
	Weight, lb (kg)								
Top hat	---- (----)	----- (----)	0.97 (0.44)	0.88 (0.40)	0.90 (0.41)	1.00 (0.45)	1.19 (0.54)	1.44 (0.65)	17.24 (1.60)
Upper hemisphere	2.63 (1.19)	6.0 (2.72)	3.62 (1.64)	3.5 (1.59)	3.63 (1.65)	3.81 (1.73)	3.44 (1.56)	3.44 (1.56)	75.4 (7.00)
Inside cone	---- (----)	----- (----)	1.14 (.52)	1.15 (.52)	1.15 (.52)	1.75 (.79)	1.87 (.85)	1.72 (.78)	44.16 (4.10)
Outside cone	1.25 (.57)	1.25 (.57)	3.27 (1.48)	3.27 (1.48)	3.27 (1.48)	3.25 (1.47)	2.81 (1.27)	3.13 (1.42)	49.69 (4.61)
Lower hemisphere	4.25 (1.93)	7.65 (3.47)	4.30 (1.95)	3.79 (1.72)	4.71 (2.14)	4.5 (2.04)	5.00 (2.27)	5.50 (2.49)	78.7 (7.31)
Sump	---- (----)	----- (----)	.34 (.15)	.38 (.17)	.41 (.19)	.88 (.40)	.56 (.25)	.62 (.28)	7.34 (.68)
Total	8.13 (3.69)	14.90 (6.76)	13.64 (6.19)	12.97 (5.88)	14.07 (6.38)	15.19 (6.89)	14.87 (6.75)	15.85 (7.19)	272.53 (25.32)

Test configuration number of blankets	Weight/area (multilayer only), lb/ft^2 (kg/m^2)	Weight/area (multilayer, bag, substrate), lb/ft^2 (kg/m^2)	Total system weight, lb (kg)
3	0.149 (0.728)	0.233 (1.14)	63.7 (28.9)
4	.205 (1.00)	.289 (1.41)	78.9 (35.8)
5	.259 (1.27)	.343 (1.68)	93.8 (42.5)
6	.317 (1.55)	.402 (1.96)	109.6 (49.7)

TABLE II. - HEAT FLOWS AND INTERNAL

Test	Total steady-state test time, hr	Boiloff rate (actual), $\dot{\omega}$, $\frac{lb}{sec}$ $\left(\frac{kg}{sec}\right)$	Prime heat input terms to LH_2 propellant						
			Heat leak through plumbing connections, QPIPES, $\frac{Btu}{sec}$ $\left(\frac{J}{sec}\right)$	Heat leak through support cone, QCONE, $\frac{Btu}{sec}$ $\left(\frac{J}{sec}\right)$	Heat leak through instrument wires, QWIRES, $\frac{Btu}{sec}$ $\left(\frac{J}{sec}\right)$	Heat given off by internal tank instrumentation, QLLS, $\frac{Btu}{sec}$ $\left(\frac{J}{sec}\right)$	Heat released due to cooling of tank wall, DTANK, $\frac{Btu}{sec}$ $\left(\frac{J}{sec}\right)$	Heat absorbed by insulation system, DINSUL, $\frac{Btu}{sec}$ $\frac{J}{sec}$	Heat leak through insulation system, QINSUL, $\frac{Btu}{sec}$ $\left(\frac{J}{sec}\right)$
3-1	2.67	0.000120 (0.000054)	0.000804 (0.847697) [a]2.71	0.007383 (7.78427) [a]24.86	0.004062 (4.28277) [a]13.68	0.003038 (3.20312) [a]10.23	0.000034 (0.035848) [a]0.10	-------- (-------)	0.014379 (15.1605) [a]48.41
3-2	10.33	0.000121 (0.000055)	0.000824 (0.868784) [a]2.89	0.007181 (7.57129) [a]25.20	0.003966 (4.18155) [a]13.92	0.002720 (2.86783) [a]9.55	-------- (--------)	0.001557 (1.64162) [a]5.46	0.012245 (12.9105) [a]42.98
3-3	10.00	0.000141 (0.000064)	0.000918 (0.967893) [a]2.59	0.008006 (8.44113) [a]22.55	0.004202 (4.43038) [a]11.84	0.003040 (3.20522) [a]8.56	0.000030 (0.031631) [a]0.08	-------- (-------)	0.019303 (20.3521) [a]54.38
R3	7.98	0.000175 (0.000079)	0.000713 (0.751752) [a]1.69	0.008609 (9.07690) [a]20.35	0.003957 (4.17206) [a]9.35	0.002831 (2.98487) [a]6.69	0.000008 (0.008435) [a]0.02	0.002094 (2.20781) [a]4.95	0.024096 (25.4056) [a]56.95
4	15.33	0.000122 (0.000055)	0.000609 (0.642099) [a]1.99	0.007852 (8.27876) [a]25.62	0.003705 (3.90637) [a]12.09	0.002725 (2.87310) [a]8.89	-------- (--------)	-------- (-------)	0.015754 (16.6102) [a]51.41
5	18.17	0.000127 (0.000058)	0.000666 (0.702197) [a]2.13	0.008037 (8.47381) [a]25.66	0.003917 (4.12989) [a]12.50	0.002722 (2.86994) [a]8.69	-------- (--------)	-------- (-------)	0.015983 (16.8517) [a]51.02
6	15.75	0.000120 (0.000054)	0.000669 (0.705360) [a]2.26	0.008072 (8.51071) [a]27.28	0.003807 (4.01391) [a]12.87	0.002880 (3.03653) [a]9.73	0.000007 (0.007380) [a]0.02	0.000561 (0.591490) [a]1.90	0.013589 (14.3276) [a]45.93

[a]Percentages.

ENERGY CHANGES FOR SPACE-HOLD TESTS

Sum of all prime heat input terms to propellant and insulation system, $\frac{Btu}{sec}$ $\left(\frac{J}{sec}\right)$	Latent and sensible heat contained in boiloff gas, QOUT, $\frac{Btu}{sec}$ $\left(\frac{J}{sec}\right)$	Heat absorbed by ullage gas, DULL, $\frac{Btu}{sec}$ $\left(\frac{J}{sec}\right)$	Heat absorbed by tank wall, DTANK, $\frac{Btu}{sec}$ $\left(\frac{J}{sec}\right)$	Heat released due to insulation cooling, DINSUL, $\frac{Btu}{sec}$ $\left(\frac{J}{sec}\right)$	Test tank pressure, PTANK, psia $\left(\frac{N}{m^2}\text{ abs}\right)$	Environmental chamber wall temperature, TEW, ^{o}R (K)
0.029700 (31.3142)	0.027562 (29.0600)	0.000273 (0.287838)	-------- (--------)	0.001866 (1.96742)	19.774 ($1.36 \cdot 10^5$)	473 (262.8)
0.028493 (30.0416)	0.028258 (29.7938)	0.000227 (0.239337)	0.000008 (0.008435)	-------- (-------)	16.746 ($1.16 \cdot 10^5$)	480 (266.7)
0.035499 (37.4284)	0.033202 (35.0065)	0.000263 (0.277294)	-------- (--------)	0.002034 (2.14455)	16.674 ($1.15 \cdot 10^5$)	509 (282.8)
0.042308 (44.6074)	0.041976 (44.2574)	0.000332 (0.350044)	-------- (--------)	-------- (-------)	16.565 ($1.14 \cdot 10^5$)	529 (293.9)
0.030645 (32.3106)	0.029385 (30.9821)	0.000231 (0.243555)	0.000004 (0.004217)	0.001025 (1.08071)	16.589 ($1.14 \cdot 10^5$)	515 (286.1)
0.031325 (33.0275)	0.030570 (32.2315)	0.000235 (0.247772)	0.000008 (0.008435)	0.000512 (0.539827)	16.587 ($1.14 \cdot 10^5$)	535 (297.2)
0.029585 (31.1929)	0.029354 (30.9494)	0.000232 (0.244609)	-------- (--------)	-------- (--------)	16.606 ($1.15 \cdot 10^5$)	537 (298.3)

TABLE III. - ACTUAL AND SCALED

(a) Top hat and upper

Test	Actual boundary temperatures						
	Heat leak through total top half of tank insulation, $\frac{QINSUL}{2}$, $\frac{Btu}{sec}$ $\left(\frac{J}{sec}\right)$	Calculated radiation and conduction through top hat, $\frac{Btu}{sec}$ $\left(\frac{J}{sec}\right)$	Internal energy change of top hat assembly, $\frac{Btu}{sec}$ $\left(\frac{J}{sec}\right)$ (a)	Heat flow through uninterrupted portion of top half of tank insulation, $\frac{Btu}{sec}$ $\left(\frac{J}{sec}\right)$	Heat flow per unit area, $\frac{Btu}{(hr)(ft^2)}$ $\left(\frac{J}{(hr)(m^2)}\right)$	Ideal radiation component, $\frac{Btu}{sec}$ $\left(\frac{J}{sec}\right)$	Conduction component, $\frac{Btu}{sec}$ $\left(\frac{J}{sec}\right)$
3-1	0.007189 (7.57972)	0.000160 (0.168696)	-0.000816 (-0.860350)	0.006213 (6.55068)	0.2966 (3.366×10^3)	0.000840 (0.885654)	0.005373 (5.66508)
3-2	.006123 (6.45579)	.000188 (.198218)	+.000205 (+.216142)	.006140 (6.47371)	.2931 (3.326×10^3)	.000923 (.973165)	.005217 (5.50060)
3-3	.009651 (10.1755)	.000309 (.325794)	-.002149 (-2.26580)	.007193 (7.58394)	.3434 (3.897×10^3)	.001138 (1.19985)	.006055 (6.38415)
R3	.012048 (12.7028)	.000181 (.190837)	+.000098 (+.103326)	.011965 (12.6153)	.5713 (6.484×10^3)	.001344 (1.41705)	.010621 (11.1984)
4	.007877 (8.30512)	.000110 (.115979)	+.000187 (+.197164)	.007954 (8.38630)	.3798 (4.310×10^3)	.000910 (.959459)	.007044 (7.42691)
5	.007992 (8.42637)	.000094 (.099109)	-.000199 (-.209816)	.007699 (8.11744)	.3676 (4.172×10^3)	.000838 (.883545)	.006861 (7.23396)
6	.006795 (7.16431)	.000114 (.120196)	-.000878 (-.925719)	.005803 (6.11839)	.2771 (3.145×10^3)	.000696 (.733828)	.005107 (5.38462)

(b) Bottom hat and lower

Test	Actual boundary temperatures						
	Heat leak through total bottom half of tank installation, $\frac{QINSUL}{2}$, $\frac{Btu}{sec}$ $\left(\frac{J}{sec}\right)$	Calculation radiation and conduction through sump cover, $\frac{Btu}{sec}$ $\left(\frac{J}{sec}\right)$	Internal energy change of sump cover assembly, $\frac{Btu}{sec}$ $\left(\frac{J}{sec}\right)$ (a)	Heat flow through uninterrupted portion of bottom half of tank insulation, $\frac{Btu}{sec}$ $\left(\frac{J}{sec}\right)$	Heat flow per unit area, $\frac{Btu}{(hr)(ft^2)}$ $\left(\frac{J}{(hr)(m^2)}\right)$	Ideal radiation component, $\frac{Btu}{sec}$ $\left(\frac{J}{sec}\right)$	Conduction component, $\frac{Btu}{sec}$ $\left(\frac{J}{sec}\right)$
3-1	0.007189 (7.57972)	0.000096 (0.101218)	-0.000023 (-0.024250)	0.007070 (7.45425)	0.3234 (3.670×10^3)	0.000859 (0.905687)	0.006211 (6.54863)
3-2	.006123 (6.45579)	.000136 (.143392)	+.000519 (+.547208)	.006506 (6.85960)	.2976 (3.377×10^3)	.000920 (.970002)	.005586 (5.88966)
3-3	.009651 (10.1755)	.000136 (.143392)	-.000495 (-.521903)	.009020 (9.51024)	.4126 (4.683×10^3)	.001148 (1.21039)	.007872 (8.29992)
R3	.012048 (12.7028)	.000100 (.105435)	+.000673 (+.709578)	.012621 (13.3070)	.5773 (6.552×10^3)	.001304 (1.37487)	.011317 (11.9322)
4	.007877 (8.30512)	.000108 (.113870)	-.000075 (-.079076)	.007694 (8.11217)	.3519 (3.994×10^3)	.000918 (.967893)	.006776 (7.14434)
5	.007992 (8.42637)	.000075 (.079076)	-.000029 (-.030576)	.007888 (8.31671)	.3607 (4.094×10^3)	.000848 (.894089)	.007040 (7.42269)
6	.006795 (7.16431)	.000071 (.074859)	-.000134 (-.141283)	.006590 (6.94817)	.3015 (3.422×10^3)	.000714 (.752806)	.005876 (6.19542)

[a]Minus sign indicates cooling; plus sign indicates warming.

UP HEAT FLOW VALUES

hemisphere of tank

Radiation scale up factor	Conduction scale up factor	528° R (293.3 K) boundary temperatures			
		Ideal radiation component, Btu/sec (J/sec)	Conduction component, Btu/sec (J/sec)	Heat flow through uninterrupted portion of top half of tank insulation, Btu/sec (J/sec)	Heat flow per unit area, Btu/(hr)(ft²) (J/(hr)(m²))
1.619	1.139	0.001360 (1.43393)	0.006122 (6.45479)	0.007482 (7.88872)	0.3572 (4.054×10^3)
1.473	1.110	.001360 (1.43393)	.005793 (6.10791)	.007153 (7.54184)	.3415 (3.876×10^3)
1.195	1.049	.001360 (1.43393)	.006354 (6.69940)	.007714 (8.13333)	.3683 (4.180×10^3)
1.011	1.003	.001360 (1.43393)	.010656 (11.2353)	.012016 (12.6692)	.5736 (6.510×10^3)
1.121	1.031	.001020 (1.07545)	.007264 (7.65887)	.008284 (8.73432)	.3955 (4.489×10^3)
.974	.993	.000816 (.860358)	.006812 (7.18230)	.007628 (8.04266)	.3642 (4.133×10^3)
.977	.994	.000680 (.716965)	.005076 (5.35193)	.005756 (6.06890)	.2748 (3.119×10^3)

hemisphere of tank

Radiation scale up factor	Conduction scale up factor	528° R (293.3 K) boundary temperatures			
		Ideal radiation component, Btu/sec (J/sec)	Conduction component, Btu/sec (J/sec)	Heat flow through uninterrupted portion of bottom half of tank insulation, Btu/sec (J/sec)	Heat flow per unit area, Btu/(hr)(ft²) (J/(hr)(m²))
1.584	1.133	0.001361 (1.43498)	0.007034 (7.41637)	0.008395 (8.85135)	0.3840 (4.358×10^3)
1.478	1.111	.001360 (1.43393)	.006208 (6.54547)	.007568 (7.97940)	.3462 (3.929×10^3)
1.184	1.047	.001360 (1.43393)	.008240 (8.68793)	.009600 (10.1219)	.4391 (4.983×10^3)
1.043	1.011	.001360 (1.43393)	.011445 (12.0672)	.012805 (13.5011)	.5857 (6.647×10^3)
1.112	1.029	.001021 (1.07650)	.006972 (7.35100)	.007993 (8.42750)	.3656 (4.149×10^3)
.962	.990	.000816 (.860358)	.006967 (7.34573)	.007783 (8.20608)	.3560 (4.040×10^3)
.952	.987	.000680 (.716965)	.005799 (6.11423)	.006479 (6.83120)	.2964 (3.364×10^3)

(c) Average scaled up heat flux data for 528° R (293.3 K) boundary temperatures

Test	Average of scaled up unit heat flux data for both halves of tank, Btu/(hr)(ft²) (J/(hr)(m²))
3-1	0.3706 (4.206×10^3)
3-2	.3437 (3.901×10^3)
3-3	.4037 (4.582×10^3)
R3	.5797 (6.579×10^3)
4	.3806 (4.319×10^3)
5	.3601 (4.087×10^3)
6	.2856 (3.241×10^3)

TABLE V. - HISTORY OF GROUND-HOLD TESTING

Test	Conditions prior to start of ground-hold test setup		Steps taken to establish 1-atm condition in chamber	Gases present immediately prior to and during ground-hold testing	
	Environmental chamber	Test tank		Substrate	Blankets
1	1 atm GN_2	Ambient temperature	----------	GHe	GN_2
2	1×10^{-5} mm Hg	LH_2 temperature	Break vacuum to 15.52 mm Hg using warm GHe. Finish breaking vacuum using warm GN_2.	GHe	GN_2
3a	1×10^{-5} mm Hg	LH_2 temperature	Break vacuum to 4.5 mm Hg using warm GHe. Finish breaking vacuum using warm GN_2.	GHe	GN_2
3b	1 atm GN_2	LH_2 temperature	(a)	GHe	GN_2
3c	1 atm GN_2	LH_2 temperature	(a)	GHe	GN_2
4	1 atm GHe	Ambient temperature	---	GHe	GHe

[a]Not applicable; chamber conditions established during test 3a.

TABLE IV. - PACKING DENSITY OF MULTILAYER INSULATION

ON TANK HEMISPHERES

Test	Number of effective shields	Thickness of insulation blankets only, in. (m)		Packing density, effective shields per inch (m)	
		Top hemisphere	Bottom hemisphere	Top hemisphere	Bottom hemisphere
3-1	28	0.681 (0.0173)	1.278 (0.0325)	41.1 (1618)	21.9 (862)
3-2	28	.681 (.0173)	1.278 (.0325)	41.1 (1618)	21.9 (862)
3-3	28	.681 (.0173)	1.278 (.0325)	41.1 (1618)	21.9 (862)
R3	28	.59 (.0150)	.60 (.0152)	47.5 (1870)	46.7 (1839)
4	37	.68 (.0173)	.67 (.0170)	54.4 (2142)	55.2 (2173)
5	46	.81 (.0206)	.83 (.0211)	56.8 (2236)	55.4 (2181)
6	55	.88 (.0224)	.97 (.0246)	62.5 (2461)	56.7 (2232)

TABLE VI. - HEAT FLOWS AND INTERNAL ENERGY

[Purges: substrate, GHe;

Test	Total steady-state test time, hr	Boiloff rate (actual), $\dot{w}$, $\frac{lb}{sec}$ $\left(\frac{J}{sec}\right)$	Prime heat input terms to LH_2 propellant					
			Heat leak through plumbing connections, QPIPES, $\frac{Btu}{sec}$ $\left(\frac{J}{sec}\right)$	Heat leak through support cone, QCONE, $\frac{Btu}{sec}$ $\left(\frac{J}{sec}\right)$	Heat leak through instrument wires, QWIRES, $\frac{Btu}{sec}$ $\left(\frac{J}{sec}\right)$	Heat given off by internal tank instrumentation, QLLS, $\frac{Btu}{sec}$ $\left(\frac{J}{sec}\right)$	Heat added by GHe substrate purge, QPURGE, $\frac{Btu}{sec}$ $\left(\frac{J}{sec}\right)$	Heat released due to cooling of tank wall, DTANK, $\frac{Btu}{sec}$ $\left(\frac{J}{sec}\right)$
1	1.33	0.018392 (0.008343)	0.001386 (1.46133) [a]0.03	0.014465 (15.2511) [a]0.30	0.006073 (6.40307) [a]0.13	0.002623 (2.76556) [a]0.05	0.088101 (92.8893) [a]1.82	-------- (-------)
2	1.00	0.023883 (0.010833)	0.001323 (1.39491) [a]0.02	0.011392 (12.0112) [a]0.19	0.005453 (5.74937) [a]0.09	0.002617 (2.75923) [a]0.04	0.082816 (87.3171) [a]1.36	-------- (-------)
3a	0.99	0.026055 (0.011819)	0.001444 (1.52248) [a]0.02	0.008210 (8.65621) [a]0.13	0.004482 (4.72560) [a]0.07	0.002699 (2.84569) [a]0.04	0.106247 (112.022) [a]1.63	-------- (-------)
3b	0.95	0.024117 (0.010939)	0.001387 (1.46238) [a]0.02	0.009173 (9.67155) [a]0.15	0.004691 (4.94596) [a]0.08	0.002617 (2.75923) [a]0.04	0.104766 (110.460) [a]1.68	-------- (-------)
3c	1.07	0.023702 (0.010751)	0.001354 (1.42759) [a]0.02	0.011365 (11.9827) [a]0.18	0.005300 (5.58806) [a]0.09	0.002632 (2.77505) [a]0.04	0.104005 (109.658) [a]1.68	-------- (-------)
4	0.27	0.029227 (0.013257)	0.001028 (1.08387) [a]0.01	0.012917 (13.6190) [a]0.16	0.004428 (4.66866) [a]0.05	0.002617 (2.75923) [a]0.03	0.098661 (104.023) [a]1.21	-------- (-------)

[a]Percentages.

CHANGES FOR GROUND-HOLD TESTS

environmental chamber, GN_2.]

Heat absorbed by insulation system, DINSUL, Btu/sec (J/sec)	Heat leak through insulation system, QINSUL, Btu/sec (J/sec)	Sum of all prime heat input terms to propellant and insulation system, Btu/sec (J/sec)	Latent and sensible heat contained in boiloff gas, QOUT, Btu/sec (J/sec)	Heat absorbed by ullage gas, DULL, Btu/sec (J/sec)	Heat absorbed by tank wall, DTANK, Btu/sec (J/sec)	Heat released due to insulation cooling, DINSUL, Btu/sec (J/sec)	Test tank pressure, PTANK, psia ($\frac{N}{m^2}$ abs)	Environmental chamber wall temperature, TEW, °R (K)
0.007878 (8.30617) [a]0.16	4.7100 (4965.99) [a]97.51	4.8305 (5093.0)	4.7840 (5044.0)	0.038770 (40.8772)	0.007906 (8.33569)	-------- (-------)	19.938 (1.37×10^5)	477 (265)
0.012995 (13.7013) [a]0.21	5.9642 (6288.35) [a]98.08	6.0808 (6411.3)	6.0194 (6346.6)	0.053184 (56.0746)	0.008246 (8.69417)	-------- (-------)	19.740 (1.36×10^5)	473 (263)
-------- (-------)	6.3956 (6743.20) [a]98.11	6.5187 (6873.0)	6.4494 (6799.9)	0.046773 (49.3151)	0.008382 (8.83756)	0.014085 (14.8505)	16.699 (1.15×10^5)	487 (271)
0.002208 (2.32801) [a]0.04	6.0964 (6427.74) [a]97.99	6.2212 (6559.3)	6.1700 (6505.3)	0.042354 (44.6559)	0.008907 (9.39110)	-------- (-------)	16.670 (1.15×10^5)	486 (270)
0.003664 (3.86314) [a]0.06	6.0530 (6381.98) [a]97.92	6.1813 (6517.3)	6.1315 (6464.7)	0.041806 (44.0782)	0.008009 (8.44429)	-------- (-------)	16.702 (1.15×10^5)	487 (271)
0.018976 (20.0073) [a]0.23	8.0217 (8457.68) [a]98.30	8.1603 (8603.8)	8.0583 (8496.3)	0.051734 (54.5457)	0.050258 (52.9895)	-------- (-------)	16.599 (1.14×10^5)	513 (285)

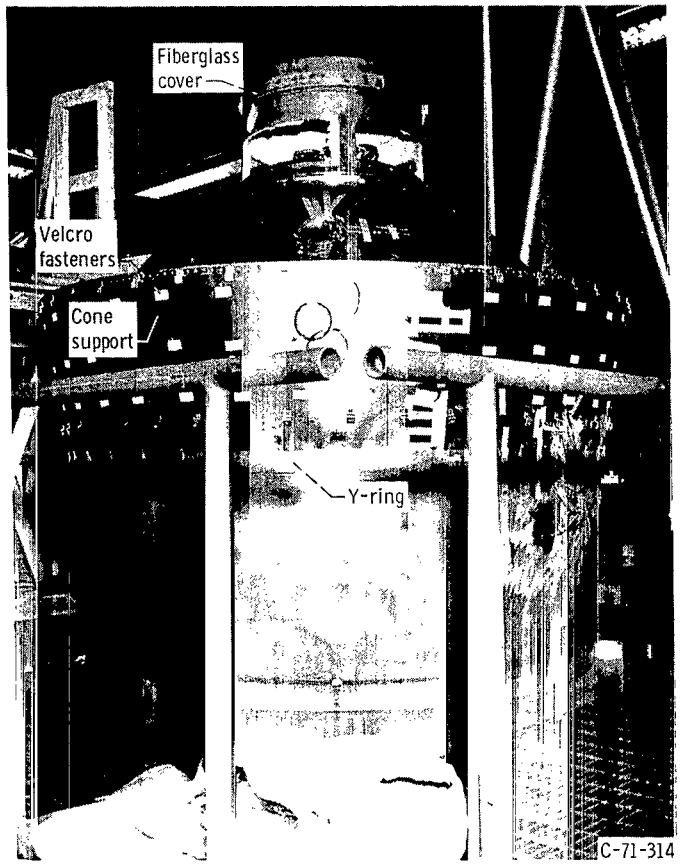

Figure 1. - Test tank and support cone.

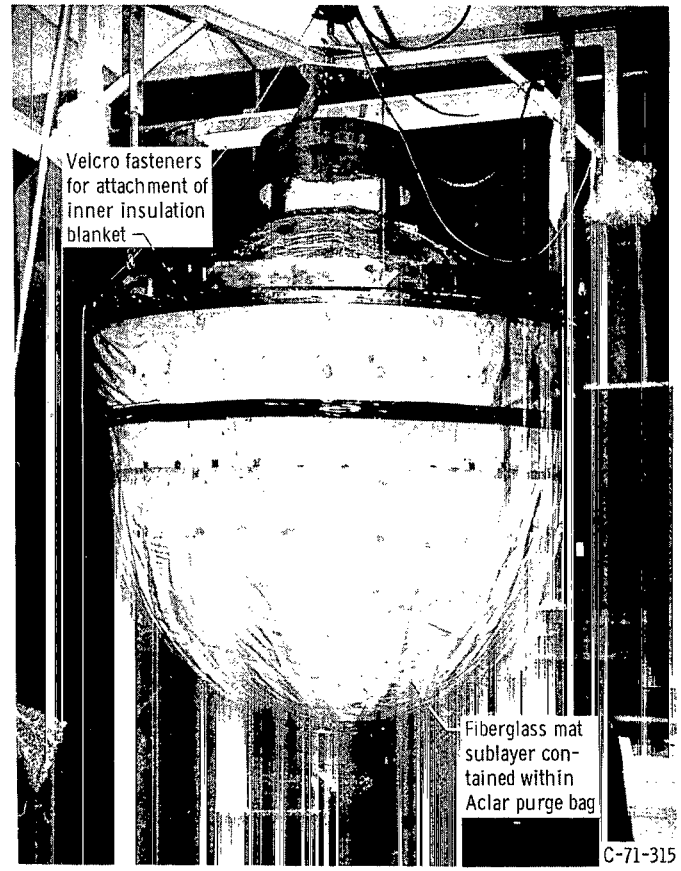

Figure 2. - Ground-hold subsystem.

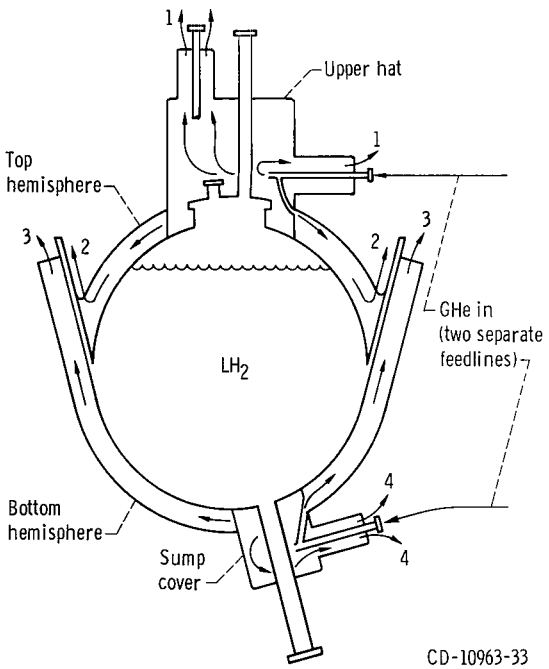

Figure 3. - Ground-hold system and helium gas purge flow paths.

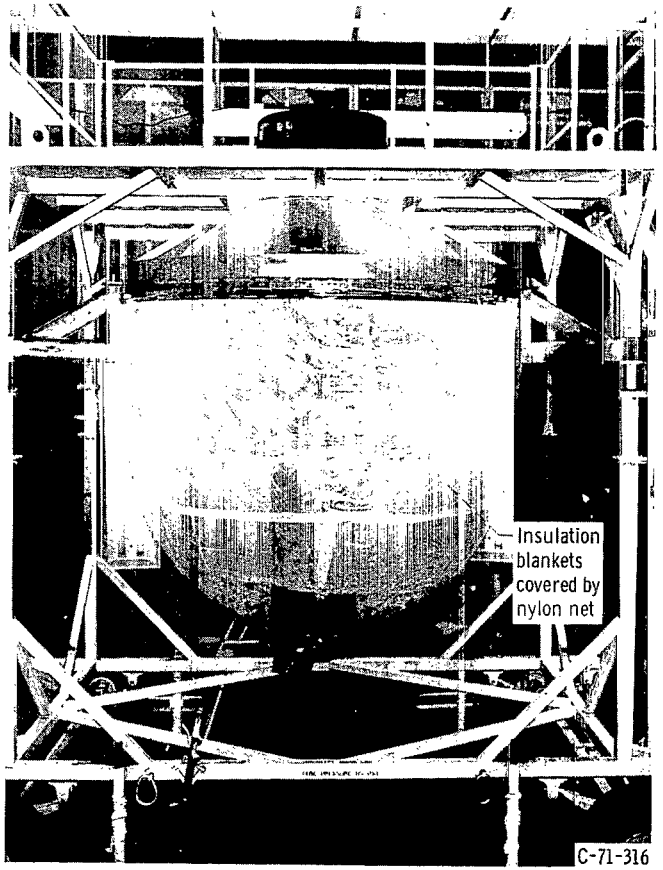

Figure 4. - Insulation blankets.

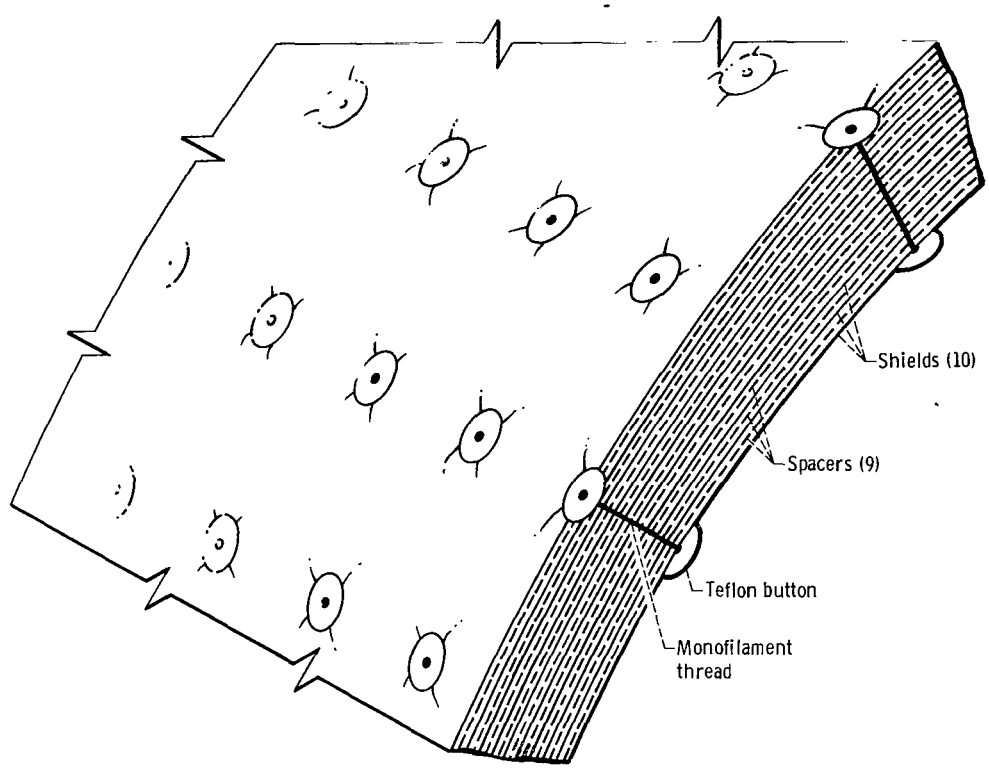

(a) Gore segment construction.

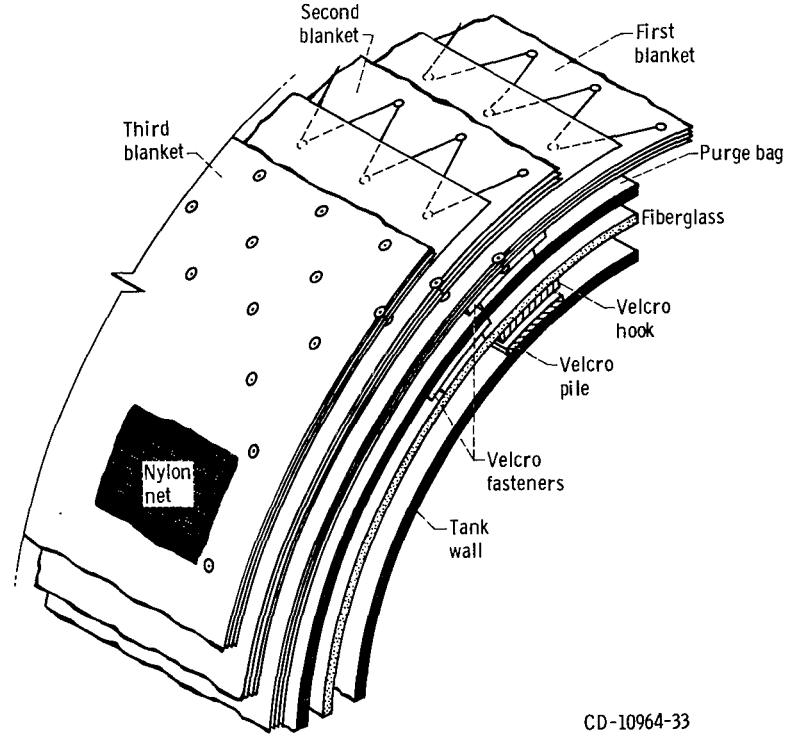

(b) System cross section on tank hemisphere.

Figure 5. - Insulation system construction.

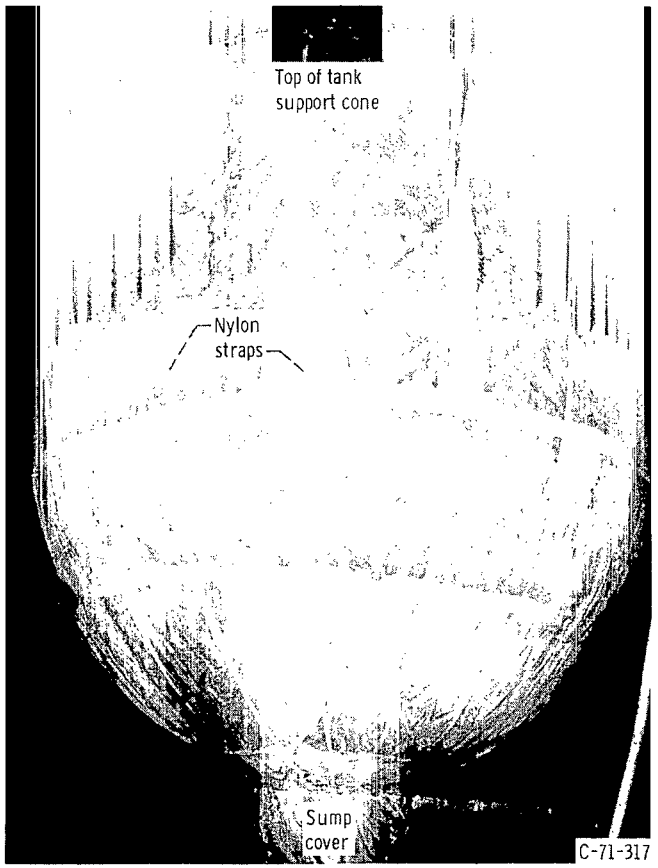

Figure 6. - Installation of fourth, fifth, and sixth blankets.

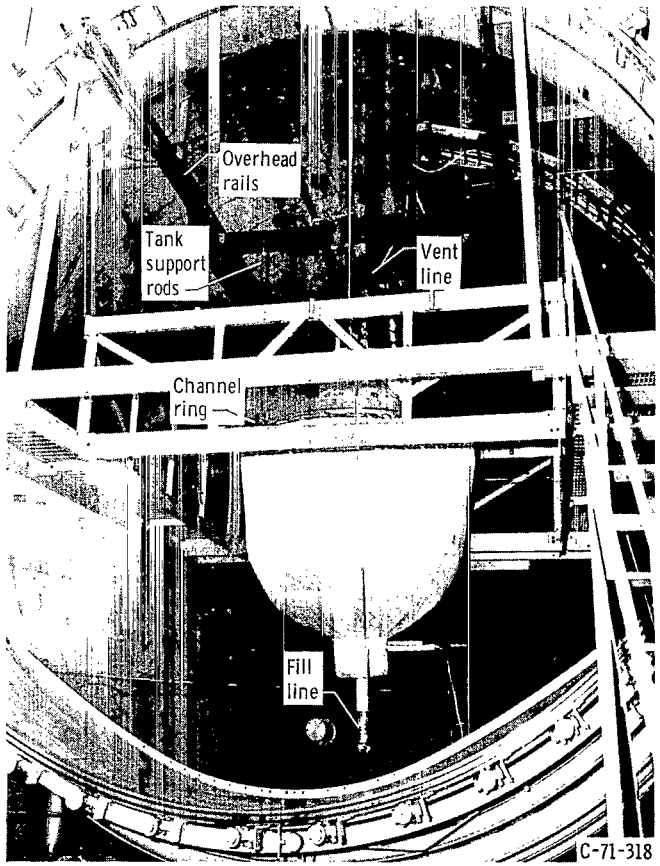

Figure 7. - Test configuration inside environmental chamber.

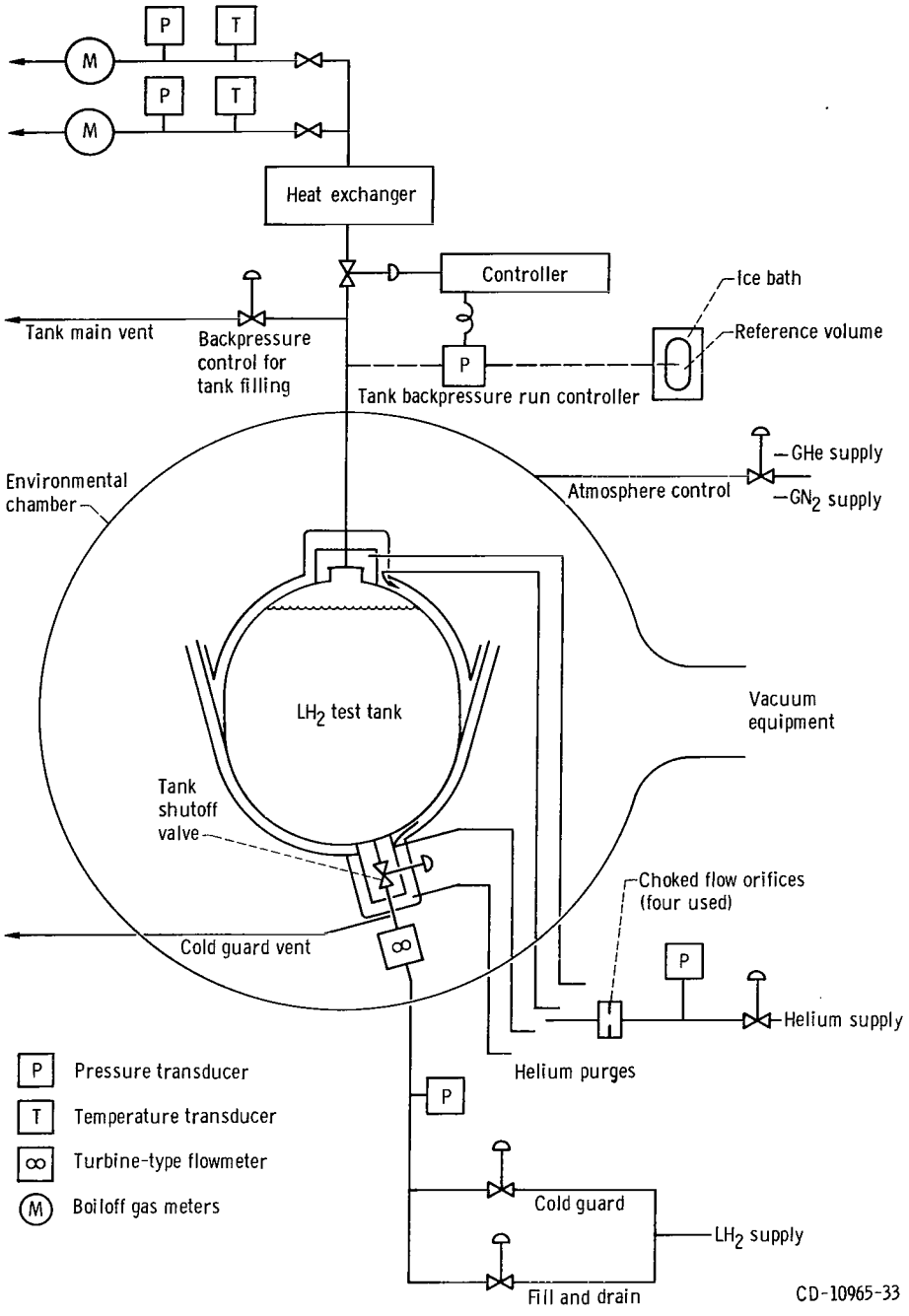

Figure 8. - General schematic of facility plumbing.

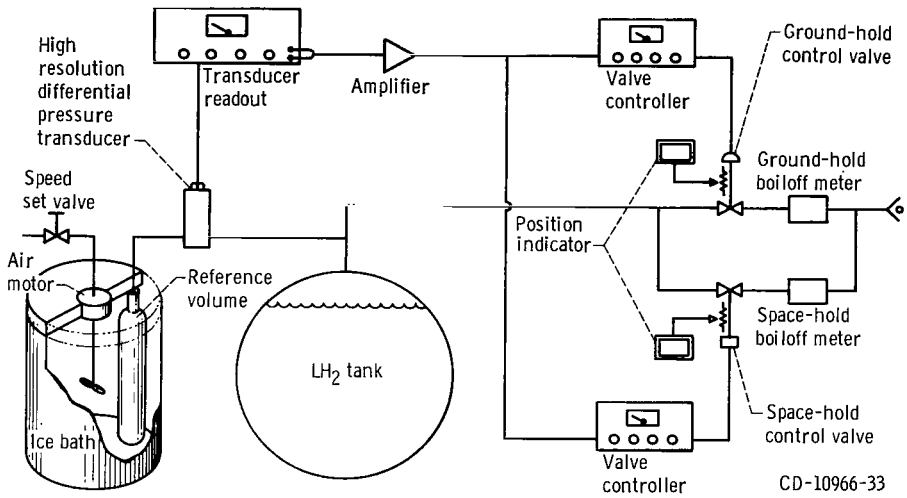

Figure 9. - Block diagram of tank backpressure control system.

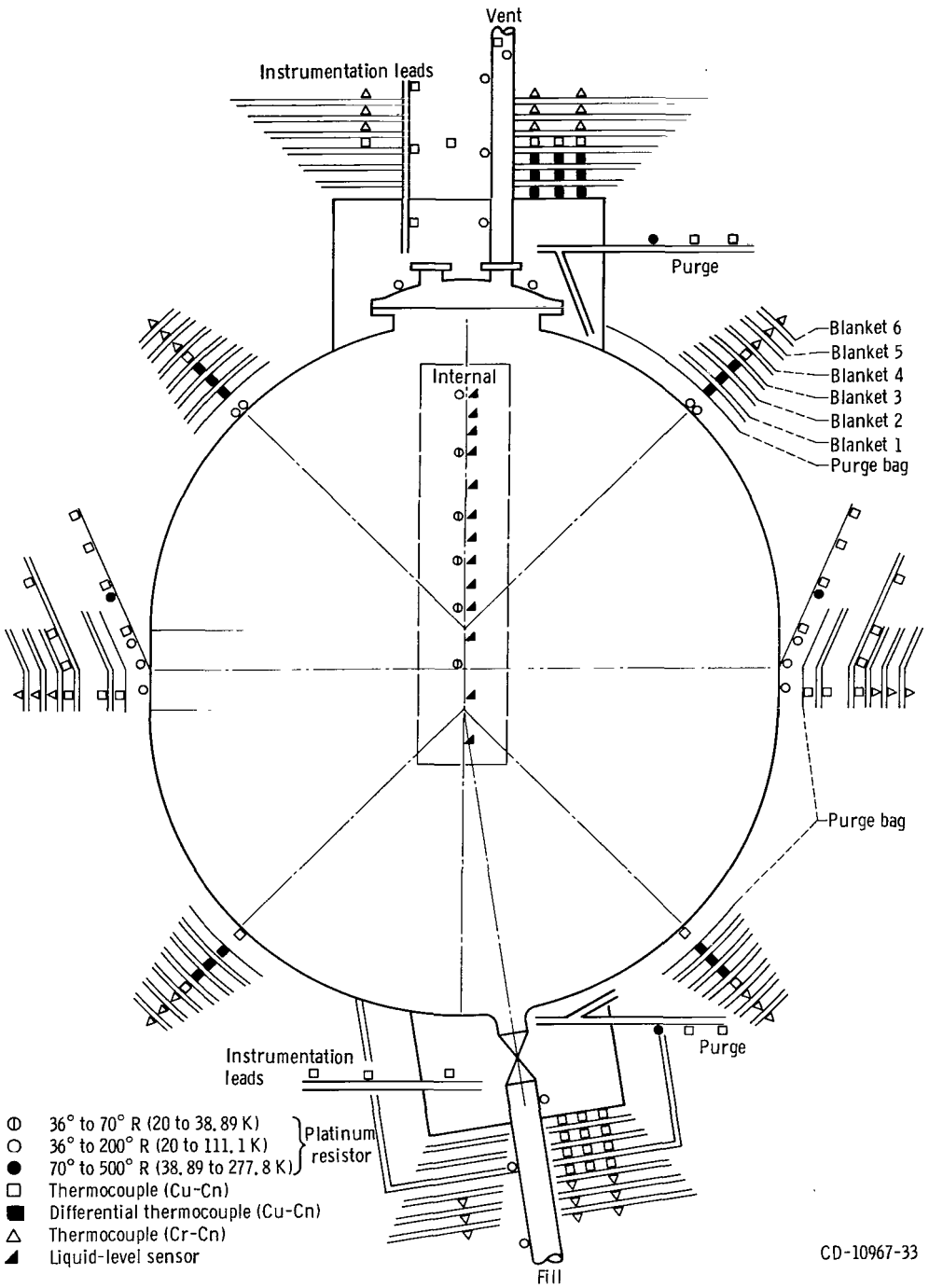

Figure 10. - Instrumentation.

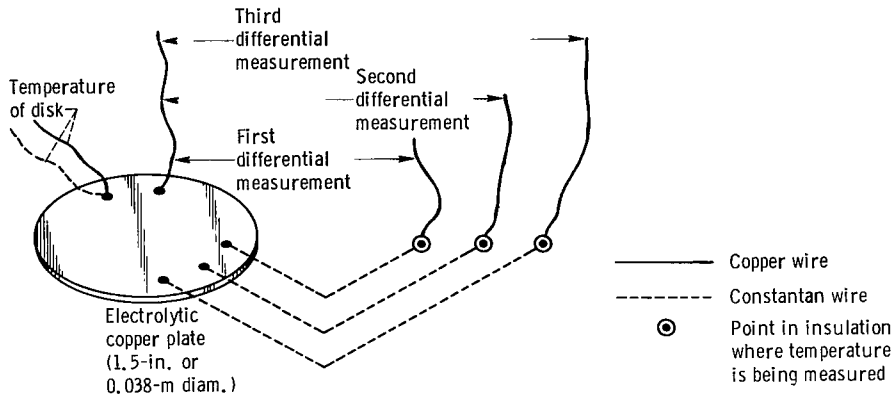

(a) Dynamic reference plate and basic thermocouple circuit.

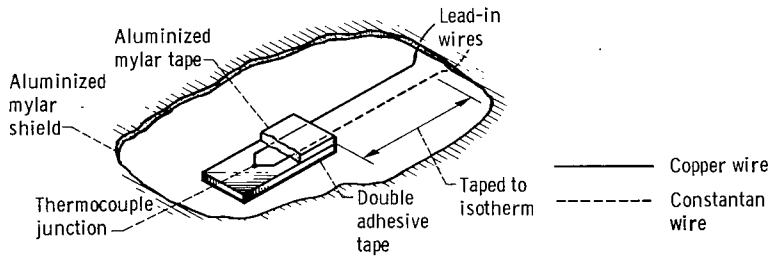

(b) Thermocouple junction installation.

CD-10968-33

Figure 11. - Differential thermocouple measurements.

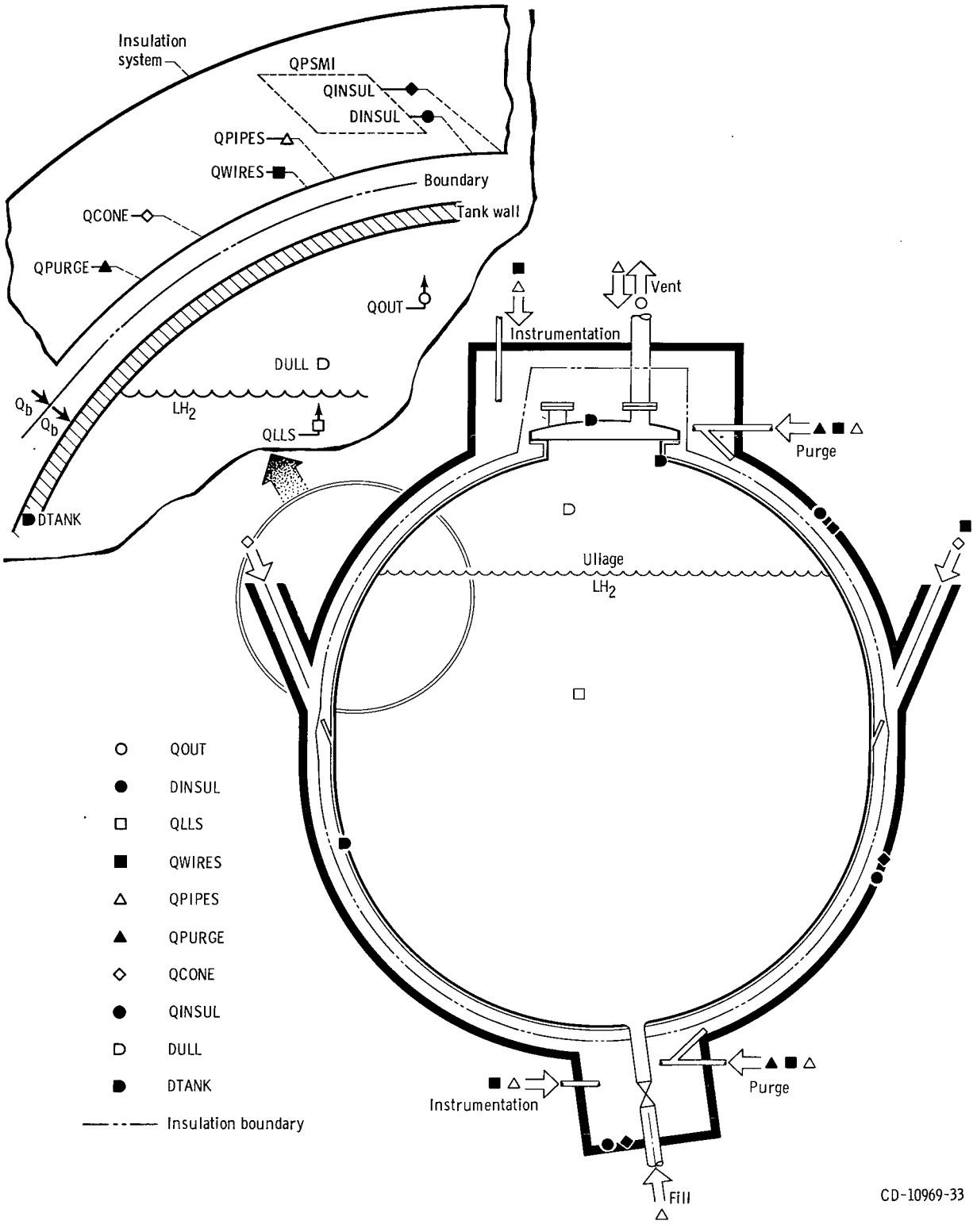

Figure 12. - Schematic representation of heat vectors.

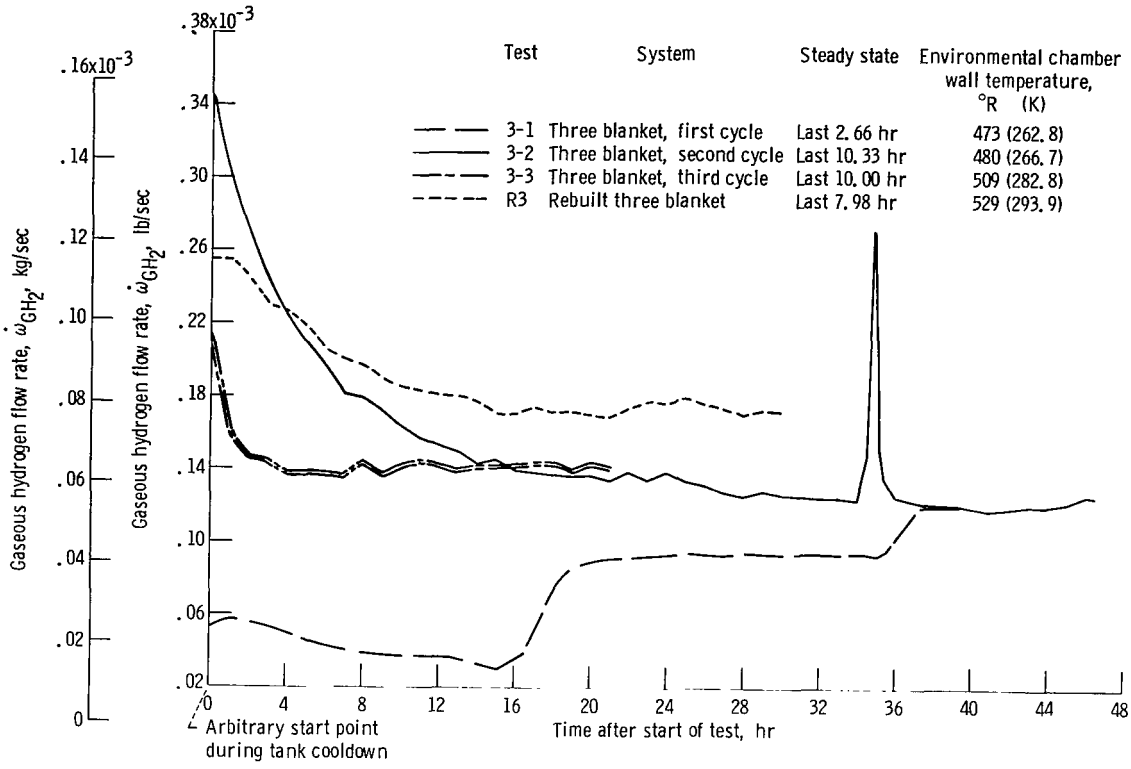

Figure 13. - Actual gaseous hydrogen boiloff plotted against test time for all three-blanket systems. (Data plot partition is 1 hr except for highly transient sections.)

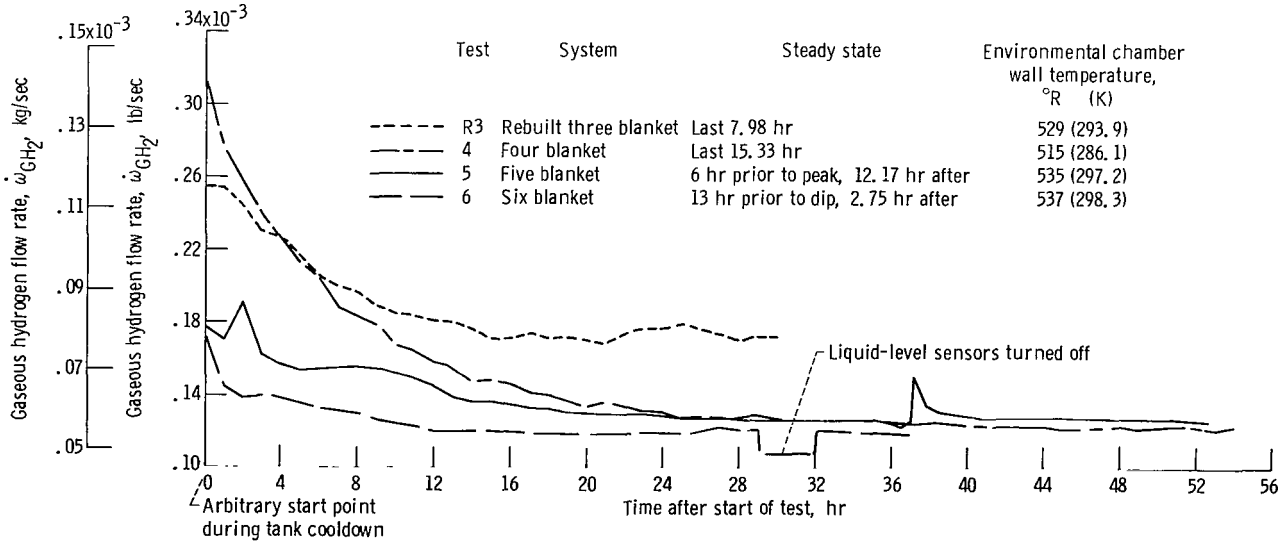

Figure 14. - Actual gaseous hydrogen boiloff plotted against test time for increasing insulation thicknesses. (Data plot partition is 1 hr except in highly transient sections.)

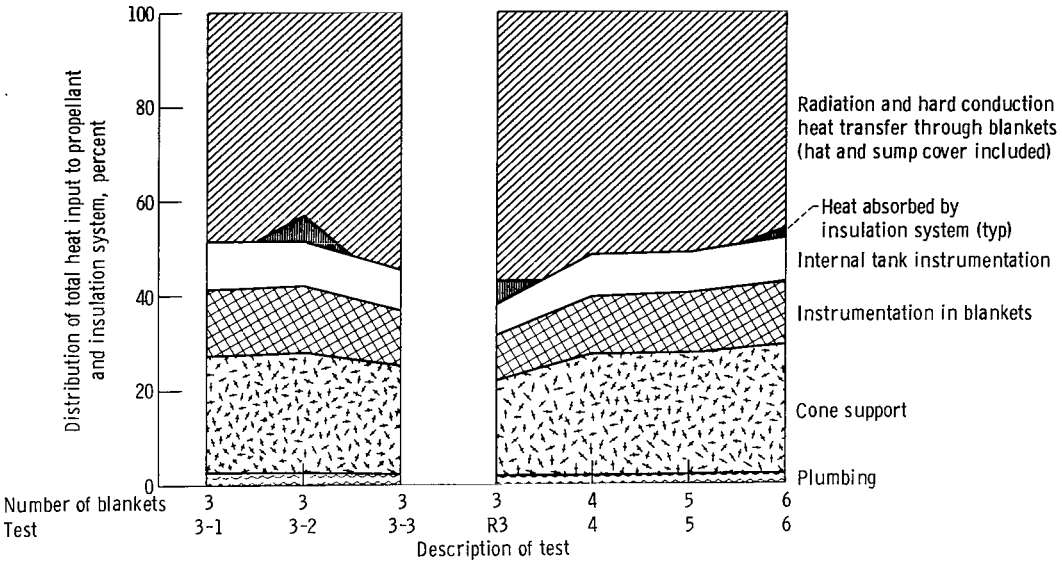

Figure 15. - Distribution of total heat input to propellant tank and insulation for 7-foot- (2.134-m-) diameter tank. Space-hold condition; actual boundary temperatures.

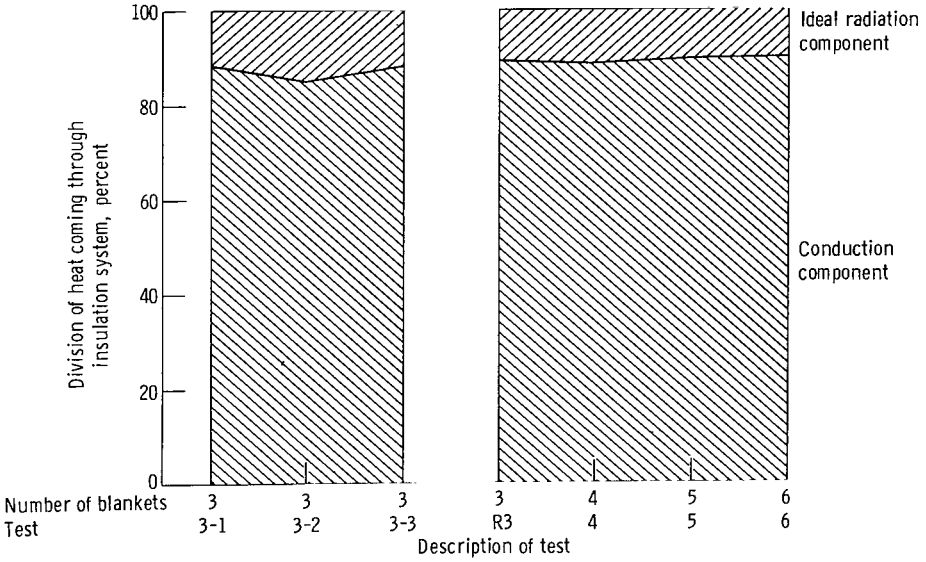

Figure 16. - Division of QINSUL plotted against test description. Space-hold condition; actual boundary temperatures.

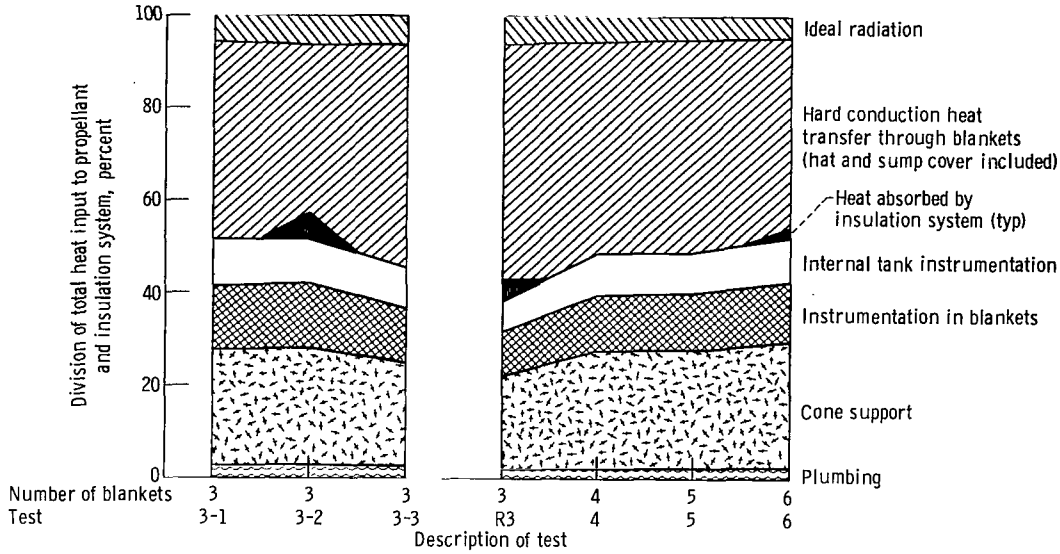

Figure 17. - Distribution of total heat input (with ideal radiation) to propellant tank and insulation for 7-foot- (2.134-m-) diameter tank. Space-hold condition; actual boundary temperatures.

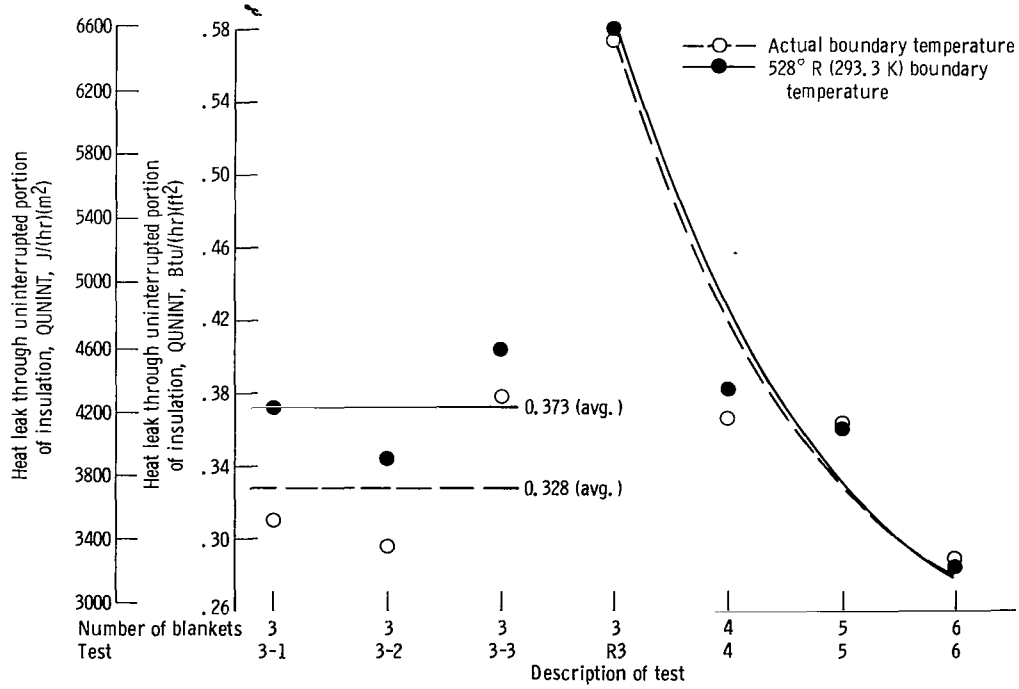

Figure 18. - Heat leak through uninterrupted portion of insulation.

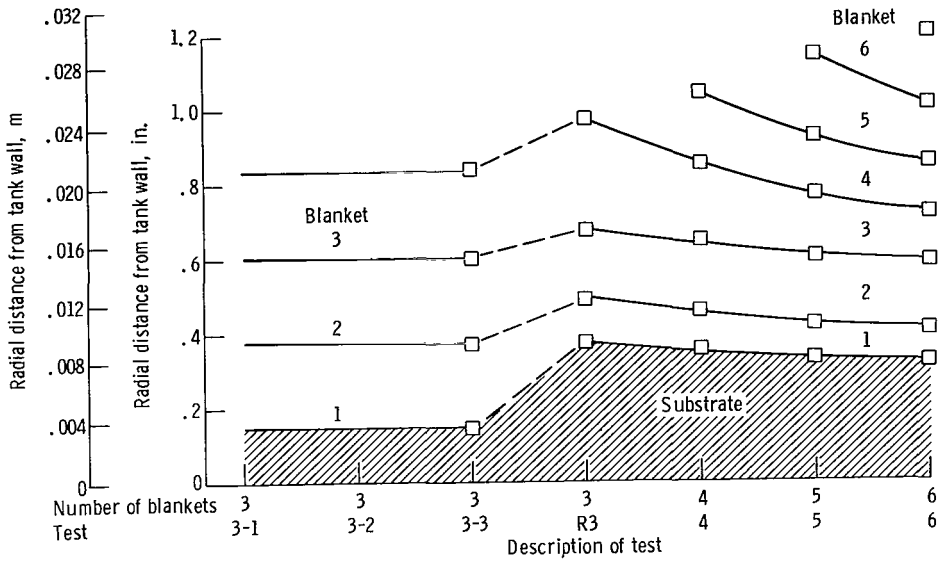

Figure 19. - Top hemisphere insulation system thickness (actual measurements from X-rays).

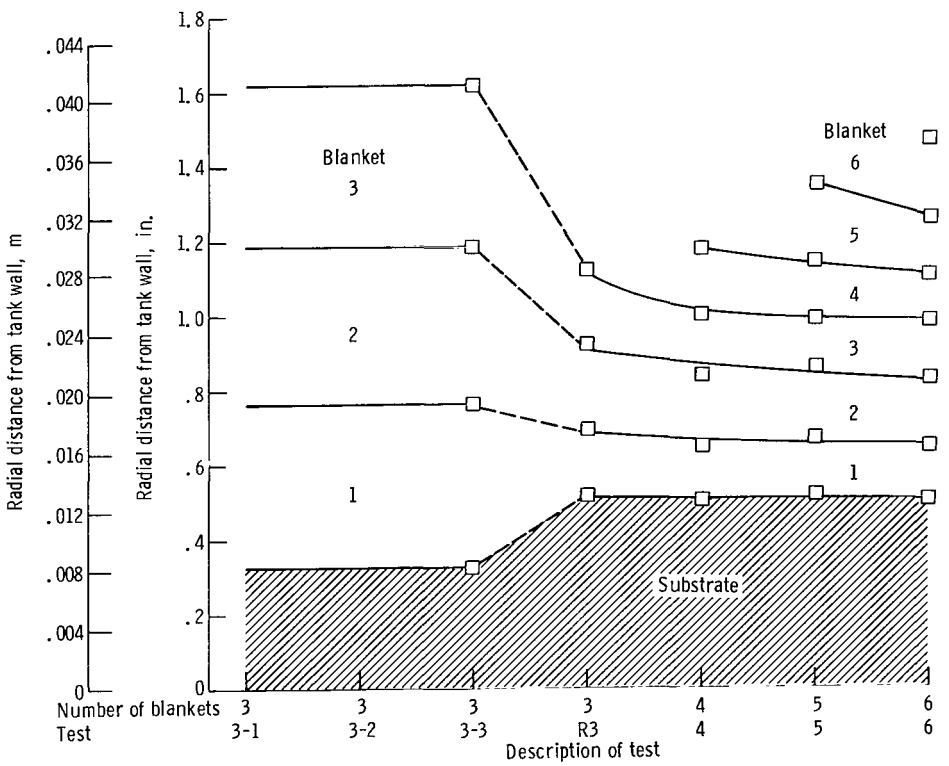

Figure 20. - Bottom hemisphere insulation system thickness (actual measurements from X-rays).

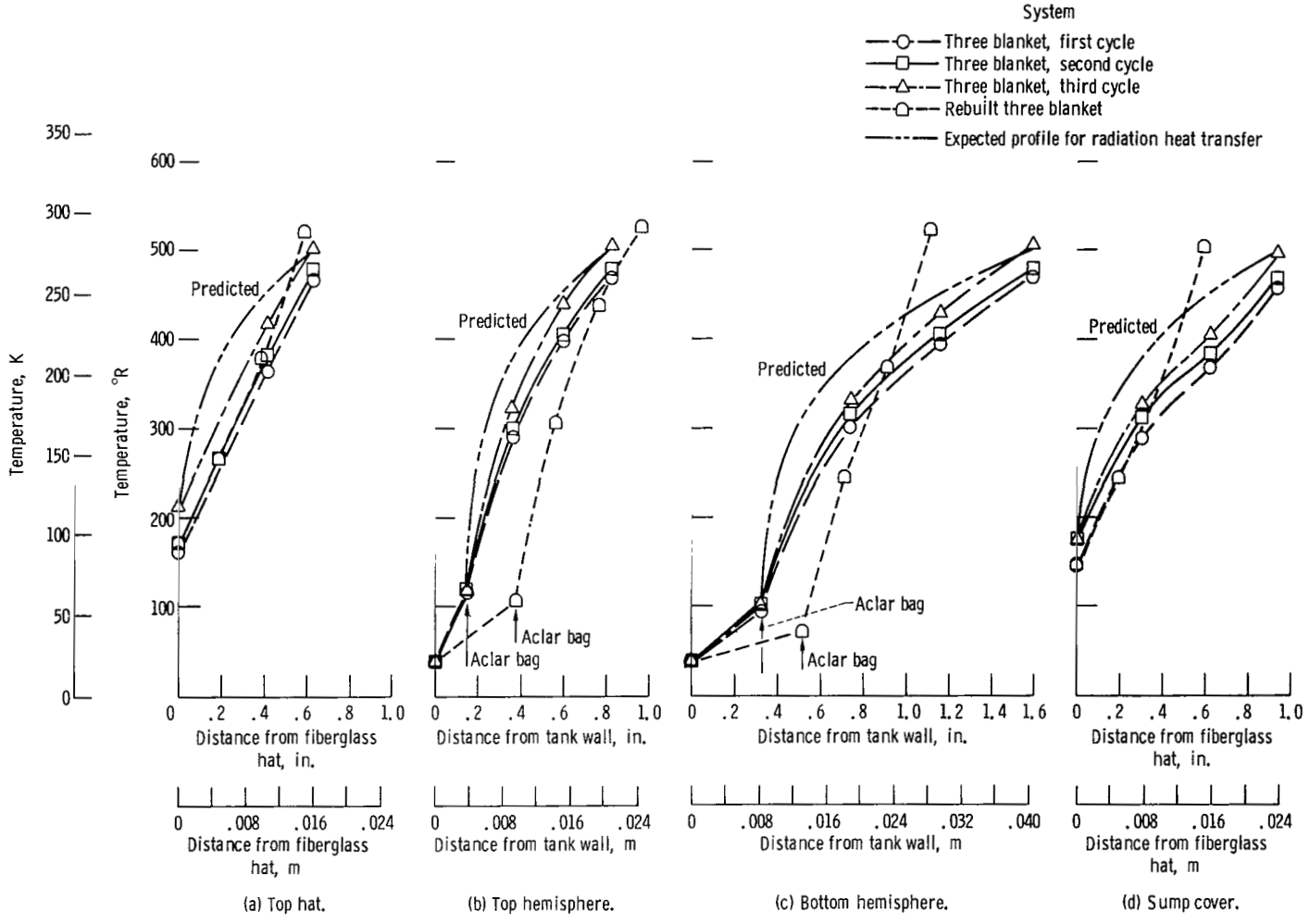

Figure 21. - Temperature profiles in three-blanket insulation system for 7-foot- (2.134-m-) diameter tank. Space-hold condition; uniform blanket distribution assumed.

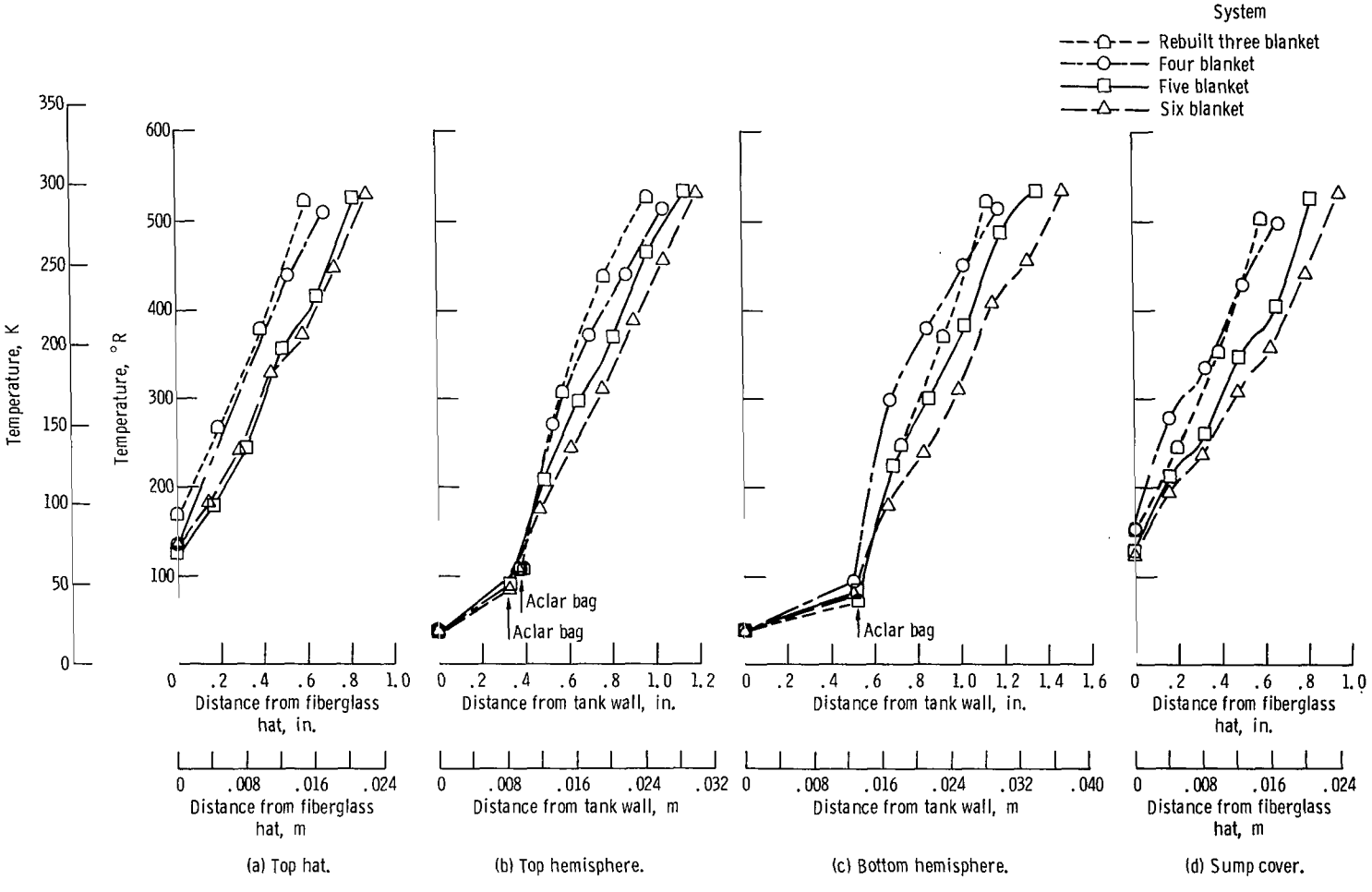

Figure 22. - Temperature profiles in three-, four-, five-, and six-blanket insulation systems for 7-foot- (2.134-m-) diameter tank. Space-hold condition; uniform blanket distribution assumed.

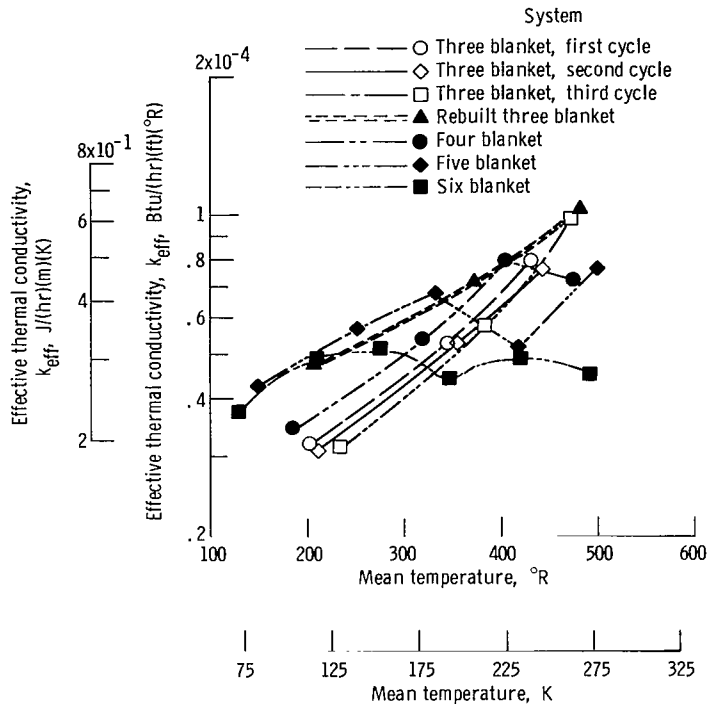

Figure 23. - Effective thermal conductivity of insulation blankets for 7-foot- (2.134-m-) diameter tank. Top hemisphere; uniform blanket distribution assumed; nonuniform boundary temperature (actual).

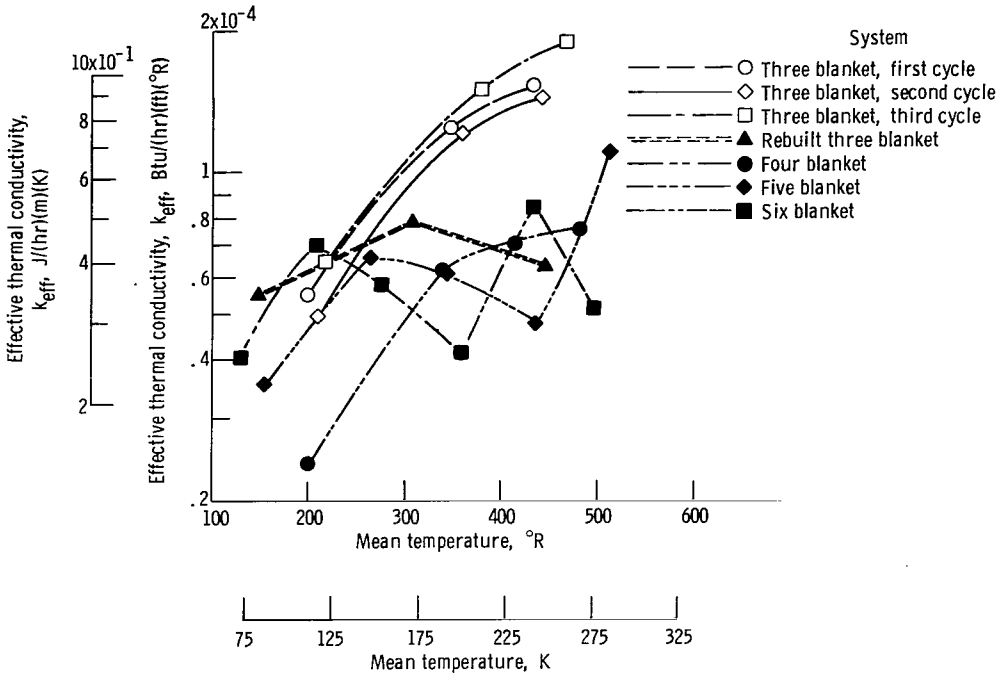

Figure 24. - Effective thermal conductivity of insulation blankets for 7-foot- (2.134-m-) diameter tank. Bottom hemisphere; uniform blanket distribution assumed; nonuniform boundary temperatures (actual).

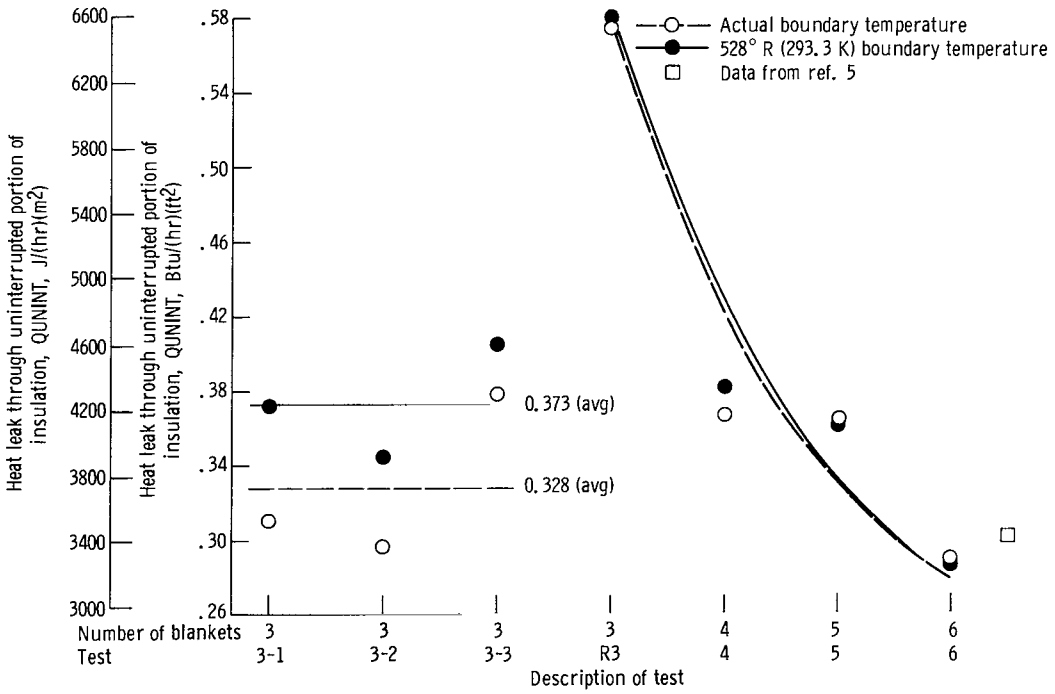

Figure 25. - Heat leak through uninterrupted portion of insulation compared with data from reference 5.

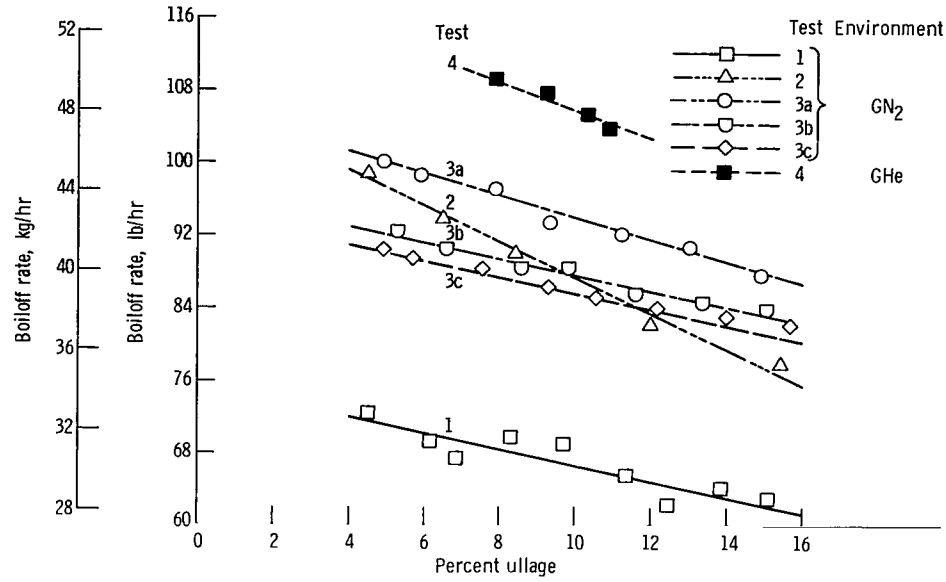

Figure 26. - Boiloff rate plotted against percent ullage. Ground-hold condition; total volume, 190.05 cubic feet (5.382 cu m).

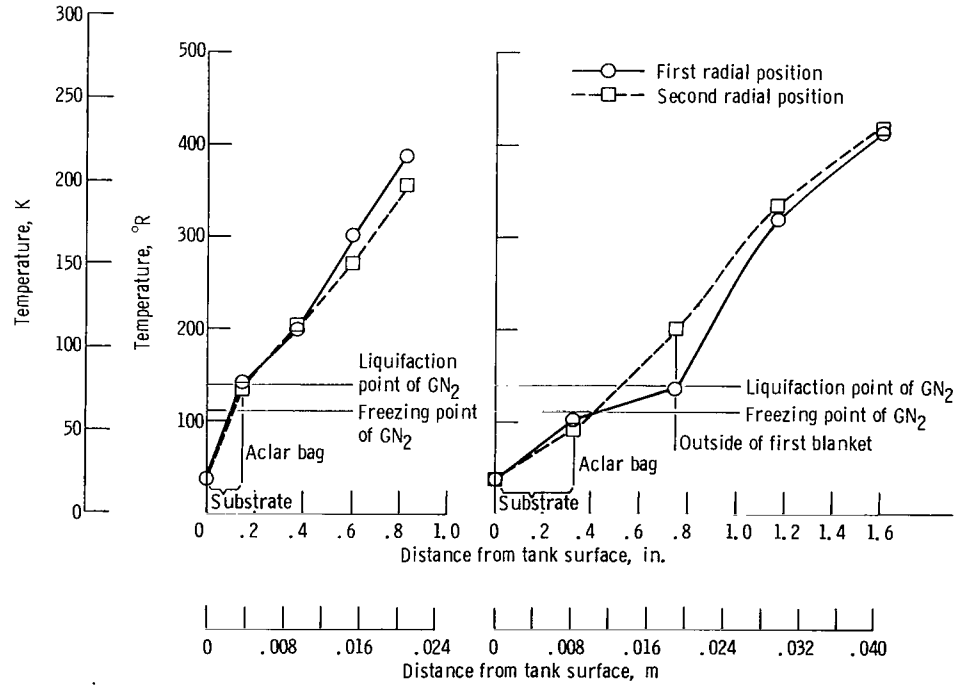

(a) Top hemisphere. (b) Bottom hemisphere.

Figure 27. - Radial temperature gradients in insulation on tank hemispheres for ground-hold test 1. Uniform blanket distribution assumed.

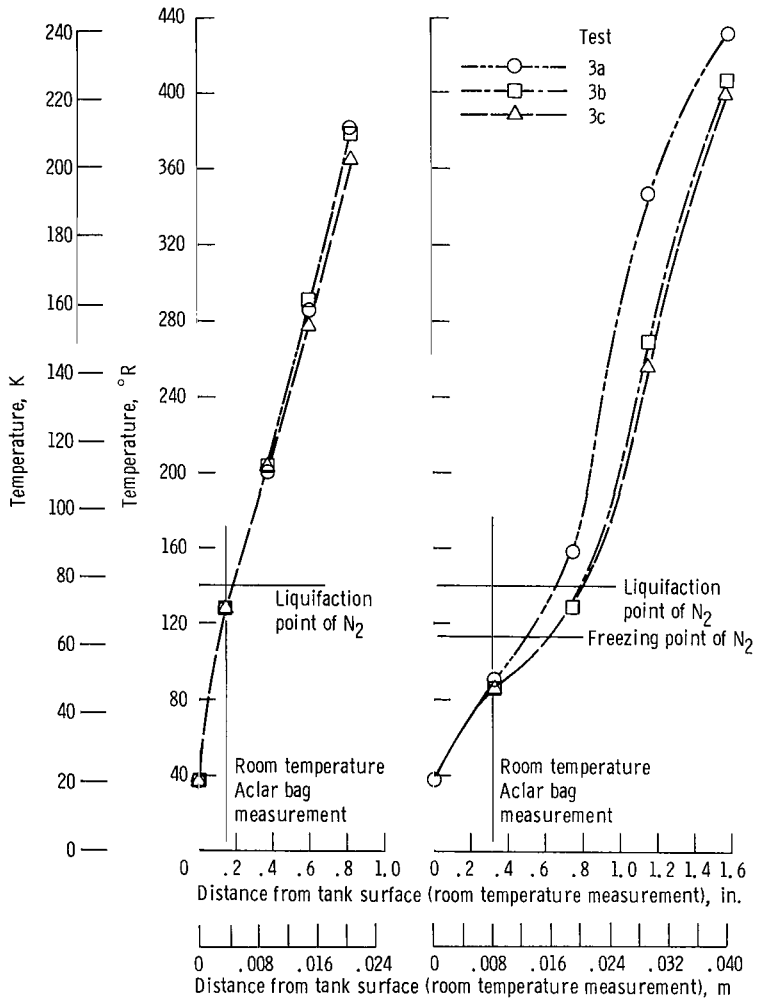

Figure 28. - Position averaged radial temperature gradients.

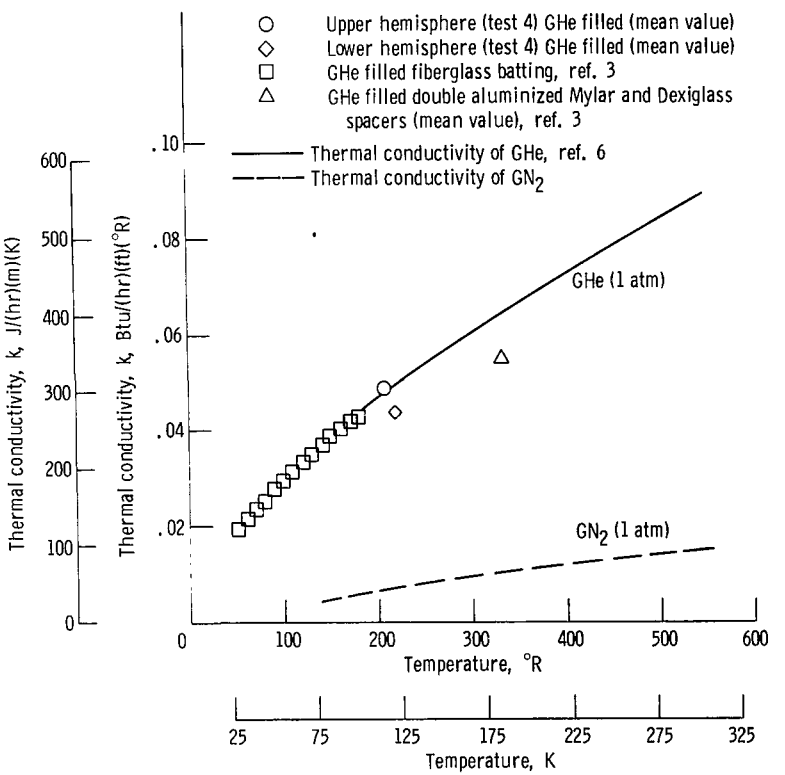

Figure 29. - Thermal conductivity of GHe filled PSMI system and of selected subsystems.

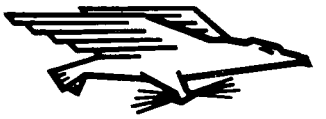

"The aeronautical and space activities of the United States shall be conducted so as to contribute . . . to the expansion of human knowledge of phenomena in the atmosphere and space. The Administration shall provide for the widest practicable and appropriate dissemination of information concerning its activities and the results thereof."

—NATIONAL AERONAUTICS AND SPACE ACT OF 1958

NASA SCIENTIFIC AND TECHNICAL PUBLICATIONS

TECHNICAL REPORTS: Scientific and technical information considered important, complete, and a lasting contribution to existing knowledge.

TECHNICAL NOTES: Information less broad in scope but nevertheless of importance as a contribution to existing knowledge.

TECHNICAL MEMORANDUMS: Information receiving limited distribution because of preliminary data, security classification, or other reasons.

CONTRACTOR REPORTS: Scientific and technical information generated under a NASA contract or grant and considered an important contribution to existing knowledge.

TECHNICAL TRANSLATIONS: Information published in a foreign language considered to merit NASA distribution in English.

SPECIAL PUBLICATIONS: Information derived from or of value to NASA activities. Publications include conference proceedings, monographs, data compilations, handbooks, sourcebooks, and special bibliographies.

TECHNOLOGY UTILIZATION PUBLICATIONS: Information on technology used by NASA that may be of particular interest in commercial and other non-aerospace applications. Publications include Tech Briefs, Technology Utilization Reports and Technology Surveys.

Details on the availability of these publications may be obtained from:

SCIENTIFIC AND TECHNICAL INFORMATION OFFICE

NATIONAL AERONAUTICS AND SPACE ADMINISTRATION

Washington, D.C. 20546